Exploring the assembly process and properties of novel crosslinker-free hyaluronate-based polyelectrolyte complex nanocarriers

Anita Umerska[a)], Krzysztof J. Paluch[a)], Iwona Inkielewicz-Stępniak[a)b)], Maria Jose Santos-Martinez[a)], Owen I. Corrigan[a)], Carlos Medina[a)], Lidia Tajber[a)]*

[a)] School of Pharmacy and Pharmaceutical Sciences, Trinity College, Dublin 2, Ireland.

[b)] Department of Medical Chemistry, Medical University of Gdansk, Poland.

*To whom correspondence should be addressed: lidia.tajber@tcd.ie, Phone: 00353 1 896 2787 Fax: 00353 1 896 2810

Abstract

The aim of this work was to study the formulation of pharmaceutically relevant polyelectrolyte complex nanoparticles (NPs) composed of hyaluronic acid (HA) and chitosan (CS) containing no crosslinkers. The influence of polymer mixing ratio, concentration and molecular weight as well as the type of counterion in chitosan salt on properties of the resulting NPs was examined. Formulations and their components were studied by laser light scattering, viscosity, infrared spectroscopy and microscopy. Physical stability, isoelectric points and cytotoxicity of selected NPs were determined.

By appropriate modification of HA molecular weight, stable and non-sedimenting NPs were successfully formed. Sonication was found to be an effective method to reduce the molecular weight of HA from 2882±25 to 176±4 kDa with no chemical changes in the HA structure observed. High molecular weight CS formed micron-sized entities at all compositions investigated. Positively and negatively charged NPs were obtained depending on the mixing ratio of the polymers, with CS glutamate NPs yielding more negatively charged particles compared to CS chloride NPs. The smallest NPs (149 ±11 nm) were formed using HA with molecular weight of 176 kDa. Cytotoxicity of NPs was dependent on environmental pH but HA was found to exert cytoprotective effects on Caco-2 cells.

Keywords: hyaluronic acid, chitosan, nanoparticle, pH titration, stability, cytotoxicity.

1. Introduction

Nanoparticles (NPs) are being extensively investigated for medical applications such as drug delivery systems, molecular diagnosis, medical imaging and tissue engineering (Emerich, Thanos, 2003). Recently, there is an increased interest in NPs composed of naturally occurring polymers such as polysaccharides or their derivatives due to their diverse structures, a large number of reactive groups, low toxicity, biodegradability and satisfactory stability (Liu et al., 2008). Such polymers are generally intended to be used solely as carriers for the delivery of bioactive substances (Janes et al., 2001), however some of the polysaccharides are known to possess pharmacological and functional properties as well. Examples of those polymers include chitosan (CS) and hyaluronic acid (HA) and their applications in nanomedicine could be multifold.

CS nanoparticles have been shown to improve the oral bioavailability of peptide and protein formulations as the positive charge of CS influences its reactivity with negatively charged surfaces, e.g. cell and mucosal membranes and it has permeability enhancing properties (Agnihotri et al., 2004). HA is present in the components of extra-cellular matrix of connective tissues and its action *in vivo* depends on the polymer size. Large (400-20,000 kDa) HA chains suppress angiogenesis and inhibit phagocytosis, while oligomeric hyaluronan fragments are angiogenic, immuno-stimulatory and inflammatory (Stern et al., 2006). Hyaluronic acid also interacts specifically with cell-surface receptors, e.g. CD44 and it has previously been used in the treatment of cancer cells over-expressing CD44 (Choi et al., 2010). Also, HA acts in synergy with CS to enhance mucoadhesion (Wadhwa et al., 2009). Thus combining HA and CS into a nanoparticle may be a useful approach to form functional and also targeted delivery systems.

Although NPs containing HA and CS have been studied (Boddohi et al., 2009; de la Fuente et al., 2008 a, b), further research is required, as to the best of our knowledge, no systematic screening of factors leading to the formation of such NPs with predictable properties has been published to date.

In many of the published investigations the use of a crosslinker (tripolyphosphate, TPP) was essential to obtain NPs (de la Fuente et al., 2008a, Oyarzun-Ampuero et al., 2009). However, high concentrations of TPP have been found to be unfavourable as TPP neutralises the positive charge of chitosan, which may lead to aggregation of such NPs (Wadhwa et al., 2009). Boddohi et al. (2009) on the other hand, managed to obtain HA/CS NPs without TPP, however aggregation of the particles was observed and NPs were recovered only after leaving the suspensions to settle overnight.

In this work we attempted to manufacture cross-linker free and stable NPs composed of only HA and CS. To achieve this goal, we comprehensively investigated the manufacturing process of HA/CS NPs including examination of polymer molecular weights, the type of chitosan salt, polymer mixing ratio and total polymer concentration. The physical stability of the nanoparticle dispersion on storage at room temperature and upon the exposure to different pH values was also examined. Cytotoxicity of selected HA/CS NPs was evaluated in the Caco-2 cell line. With the recent advent of the quality by design approach adopted by the pharma industry (ICH guideline Q8, 2009), such methodical studies will become a necessity if any nanoparticulate system is to reach to the manufacturing stage.

2. Materials and methods

2.1 Materials

Hyaluronic acid sodium salt from *Streptococcus equi sp*. was purchased from Sigma (USA). Ultrapure chitosan salts: chlorides (Protasan UP CL113 and CL213) and glutamates (Protasan UP G113 and G213) were obtained from NovaMatrix (Norway). The physicochemical properties of the various types of chitosan as well as HA "as received" are presented in Table 1. APC annexin V and propidium iodide were purchased from BD Biosciences (USA) and CellTiter 96® Non-Radioactive Cell Proliferation Assay from Promega Corporation (USA). Deuterium oxide, L-glutamic acid and cell culture reagents were provided by Sigma Aldrich (Ireland). All other reagents, chemicals and solvents were of analytical grade.

2.2. Ultrasonication

Ultrasonication of HA solutions was performed with the aid of a 130 Watt ultrasonic processor (SONICS VC130PB, Sonics and Materials Inc., USA) equipped with a probe with a diameter of 3 mm. Sonication was carried out at an amplitude of 80, which corresponds to power of 13 W. Solutions of HA were transferred into a beaker immersed in an ice bath and processed with the ultrasonic probe. The duration of the ultrasonic treatment was 10, 30 minutes, 1, 1.5, 2, 4 and 6 hours. When necessary, HA was recovered by lyophilisation (VirTis 6K freeze-dryer model EL, SP Scientific, USA) for gel permeation and cell culture experiments.

2.3 Preparation of HA/CS nanoparticles

Aqueous solutions containing 0.1 or 0.2% w/v HA of different molecular weights were prepared by sonication as described above (Section 2.2.). These solutions were

then mixed with chitosan (CS) solutions (CL113 0.1% or 0.2%, CL213, G113, G213 0.1% w/v in deionised water) at room temperature under magnetic stirring. A predefined aliquot of CS solution was added to a known volume of HA solution (the total polymer concentration was either 0.1 or 0.2% w/v) and stirring was maintained for 10 minutes to allow stabilisation of the system. A suspension of particles was instantaneously obtained upon mixing of polymer solutions.

Due to dissimilar charge mixing ratios of polymers, all figures presenting results pertinent to NPs show the chitosan fraction on the bottom X-axis and the mass mixing ratio (HA/CS) on the top X-axis.

2.4 Physicochemical characterisation of polymers

Gel Permeation Chromatography (GPC) studies were performed using an analytical system composed of an LC-10 AT VD liquid chromatograph pump system, SIL-10 AD VP autoinjector, FCV-10 AL VP low pressure gradient flow-control valve, DGU-14A degasser, a Waters 410 refractive index (RI) detector with GPC for class VP (Version 1.02) and an SCL-10A VP system controller (Shimadzu, Japan). The column used was Plaquagel –OH mixed 8 μm 300 × 7.5 mm (Polymer Laboratories Ltd., UK).

For HA samples, the composition of the mobile phase was similar to that recommended by the column's manufacturer (Varian). The mobile phase was composed of 0.2 M NaCl (substitution for $NaNO_3$) and 0.01 M NaH_2PO_4 brought to pH 7.4 with NaOH solution.

For CS, the mobile phase was composed of 0.33 M acetic acid and 0.2 M sodium acetate (adapted from Boryniec et al., 1997). The mobile phase flow rate in each case was 1 ml/min and the column and detector temperatures were set to 35 ºC. Pullulan

134 standards (PL Polymer Laboratoires, Germany), were used to construct the calibration
135 curve. Standards and samples were prepared as 0.5-1 mg/ml solutions in the mobile
136 phase and 100 µl of samples or standards were injected in triplicate. Data collection
137 and integration were accomplished using Shimadzu CLASS-VP software (version
138 6.10) with GPC for Class VP (version 1.02).
139 Quantification of glutamic acid (glutamate) was done using a method adapted from
140 Afzal et al., (2002) and it was performed using a HPLC system as described above
141 using a SPD-10A VP photodiode array UV-VIS detector (Shimadzu) instead the RI
142 detector. Samples and stock standard solution were prepared in 0.15% v/v aqueous
143 solution of trifluoroacetic acid (TFA). Chitosan chloride solution prepared at the same
144 concentration as chitosan glutamate was used as a control. 50 µl of the standard or
145 sample were injected onto the Luna 5µ C18 (2) 250 × 4.6 mm column (Phenomenex,
146 Ireland). The flow rate of 1 ml/min using a mobile phase composed of 65% v/v of the
147 aqueous phase (0.15% w/w TFA) and 35% v/v of tetrahydrofuran was employed. UV
148 detection was carried out at 220 nm. The glutamate peak had a retention time of ~2.3
149 min.
150 For HA structural investigations UV spectra of 0.1% HA solutions were recorded
151 (Alkrad et al., 2003) using a UV-1700 PharmaSpec UV-Visible spectrophotometer
152 (Shimadzu, Japan). The absorbance values were measured at wavelengths ranging
153 between 200 and 280 nm with a sampling interval of 1 nm.
154 Viscosity of polymer solutions was measured using a low frequency vibration
155 viscometer (SV-10 Vibro Viscometer, A&D Company, Limited). Samples were
156 equilibrated at 25 ºC in a water bath (Precision Scientific Reciprocal Shaking Bath
157 Model 25) prior to measurement. Three separate aliquots were prepared for each
158 sample and at least three measurements were carried out for every aliquot.

^{1}H nuclear magnetic resonance spectroscopy (^{1}H-NMR) and Fourier transform infrared spectroscopy (FTIR) of HA samples recovered by lyophilisation was carried out as described previously (Hirai et al., 1991, Tajber et al., 2009). Determination of the chloride ions was performed with a Dr Lange LCK 311 test as described earlier (Parojčić et al., 2011). The test is based on the photometric determination (λ=468 nm, Dr Lange Lasa 100 spectrophotometer, Dr. Bruno Lange GmbH, Germany) of iron(III) thiocynate concentration formed by thiocynate ions released from mercury thiocynate reacting with the chloride ions. The content of sodium counterion was determined by inductively coupled plasma–mass spectrometry (ICP-MS) (Paluch et al., 2010). A known weight of the sample was placed in a digestion vessel and reacted with 69% HNO_3 and 30% H_2O_2. The vessel was sealed and heated in a microwave digester operating at 1000 W for 20 minutes at 200 ^{o}C. The sample was then diluted with deionised water and the digest analysed by ICP-MS Varian 820.

2.5 Physicochemical characterisation of nanoparticles

The intensity-averaged mean particle size (mean particle size) and the polydispersity index of the nanoparticles were determined by Dynamic Light Scattering (DLS) with the use of 173º backscatter detection and the electrophoretic mobility values measured by Laser Doppler Velocimetry (LDV) were converted to zeta potential by the Smoluchowski equation. Both DLS and LDV measurements were done on a Zetasizer Nano series Nano-ZS ZEN3600 fitted with a 633 nm laser (Malvern Instruments Ltd., UK). Samples were placed directly into the folded capillary cells without dilutions. Each analysis was carried out at 25ºC with the equilibration time set to 5 minutes. The readings were carried out at least three times for each batch and the average values of at least three batches are presented. The results obtained were corrected for sample

viscosity (Kaszuba et al., 2008) measured as outlined above. Particle size and zeta potential of sedimenting samples was measured in the supernatant after allowing the sample to equilibrate for 24 hours.

An Orion pH meter (model 520A) equipped with an Orion Ross™ 8103SC glass body pH semi-micro electrode was used for pH measurements. The pH meter was calibrated using standard buffer solutions (Orion) of pH 4.00, 7.00 and 10.00 (±0.01).

Transmittance of NP formulations was measured using a UV-1700 PharmaSpec UV-Visible spectrophotometer (Shimadzu, Japan) at an operating wavelength of 500 nm in optically homogenous quartz cuvettes (Hellma, UK) with the light path of 10 mm.

Physical stability studies of the nanoparticle suspensions upon storage at room temperature were performed for a period of up to 4 weeks. Samples from each formulation were withdrawn periodically during studies and the particle size, zeta potential and transmittance were measured.

Particle sizer Zetasizer Nano series Nano-ZS ZEN3600 fitted with a 633 nm laser together with a MPT-2 autotitrator (Malvern Instruments Ltd., UK) were used to determine the isoelectric point of the nanoparticles. 0.1M HCl and 0.1M NaOH were used as titrants. 12 ml of the NP suspension was added initially to the sample container. Each analysis was carried out at room temperature in the automatic regime using a target pH tolerance of 0.2 units. Three particle size and three zeta potential measurements were carried out for each pH value and the sample was recirculated between repeat measurements.

FTIR studies of polymer physical mixes and lyophilised NPs were carried out as described above (Tajber et al., 2009).

To measure the glutamic acid content in NPs, the non-associated glutamate was firstly separated from NPs by a combined ultrafiltration-centrifugation technique (Amicon

209 Ultra-15, MWCO of 30 kDa; Millipore, USA). 5 ml of sample was placed in the
210 sample reservoir of a centrifugal filter device and centrifuged for 15 minutes at 4,500
211 rpm. The filtrate was collected and its volume measured. The NP suspension from the
212 sample reservoir was mixed with a predefined volume of 0.1M HCl and centrifuged
213 for 30 minutes at 13,000 rpm. After centrifugation both filtrates were assayed for the
214 content of glutamate by HPLC (as described above).
215 The amount of precipitating flocs when native HA or HA sonicated for 10 minutes
216 was used to form NPs was estimated gravimetrically. The supernatant was carefully
217 separated from the flocs by aspiration using a plastic dropper, while the remaining
218 residue was dried overnight in a vacuum oven at room temperature and weighted.
219 Morphology of nanoparticles was investigated by transmission electron microscopy
220 (TEM) and scanning electon microscopy (SEM). For TEM (Jeol 2100, Japan) the
221 samples were immobilised on copper grids and stained with either 1% w/v ammonium
222 molybdate solution for 60 seconds or 1% w/v uranyl acetate solution for 30 seconds
223 and dried overnight for viewing by TEM. SEM was carried out a Zeiss Supra Variable
224 Pressure Field Emission Scanning Electron Microscope (Germany) equipped with a
225 secondary electron detector at 2 kV. Powders were directly placed onto aluminium
226 stubs, dried for 24 hours at ambient temperature in a desiccator over silica gel and
227 sputter-coated with gold under vacuum prior to analysis.
228
229 **2.6 Cell culture studies**
230 Human colon adenocarcinoma cells (Caco-2) were obtained from European
231 Collection of Cell Cultures. Cells were cultured as a monolayer in 75 cm^2 cell culture
232 flasks in Eagle's Minimal Essential Medium (MEM), supplemented with 20% foetal
233 bovine serum, penicillin (0.006 mg/ml), streptomycin (0.01 mg/ml), gentamicin

(0.005 mg/ml), sodium bicarbonate (2.2 g/l), sodium pyruvate (0.11 g/l), pH 7.4 (adjusted with NaOH or HCl solution if necessary) at 5% CO_2 and 37º C humidified atmosphere (CO_2 incubator series 8000DH, ThermoScientific). Cells were supplied with fresh medium every second day and split after detaching with EDTA- trypsin twice a week. For experimental purposes the passage number range was maintained between 20 and 30.

2.7 MTS assay

Caco-2 cells were seeded into flat-bottom 96-well plates in 100 µl of 20% MEM at a density of 25000 cells per well (cells were previously counted with the aid of Z1 Coulter Particle Counter, Beckman Coulter) and incubated at 37 ºC for one day. The medium was then replaced with 100 µl of the sample (sonicated HA, HA/CL113) dispersed or dissolved in serum-free media. After 72 hours of incubation, or 24 h when a serum-free medium at pH 5 was used, the supernatant was removed from the wells and replaced with serum-free media. 20 µl of the MTS reagent prepared according to the manufacturer's protocol was then added into each well; for positive control (0% viability) the media was replaced by 10% SDS solution in serum-free media 30 min before the addition of MTS reagent. After 4 hours the UV absorbance of the formazan product was measured spectrophotometrically (FLUOstar Optima microplate reader, BMG Labtech) at 492 nm. The positive control was treated as a blank and its absorbance was subtracted from each reading. The cells' viability was expressed as the ratio of the absorbance value of the cells treated with different samples and that of the negative control (cells treated with serum-free (0%) MEM at pH=5.0 or pH=7.4). The negative control was assumed to have 100% of the cell viability. IC_{50} values (concentrations required to reduce the viability of cells by 50%

as compared with the control cells) were calculated by fitting the experimental points to the Hill equation using Origin software ver. 7.5.

2.8 Flow cytometry

Cell survival/ death were assayed using flow cytometry (Radziwon-Balicka et al., 2012). One 75 cm^2 flask of confluent Caco-2 cells was seeded into eight 25 cm^2 flasks, each containing Caco-2 cells suspended in 4 ml of 20% MEM. Cells were allowed to attach for 24-48 hours. The medium was then replaced with 3 ml of sample (sonicated HA). After 72 hours of incubation the supernatant was removed and cells were harvested with trypsin/EDTA. After neutralisation, the cells were combined with the previous supernatant and centrifuged (300 g, 5 minutes, Eppendorf centrifuge 5804R, Germany); the supernatant from centrifugation was discarded, and cells were washed with binding buffer (0.14M NaCl, 0.0025M $CaCl_2$ and 0.01M HEPES, pH 7.4 adjusted with NaOH solution). 20 µl of the cell suspension was stained with 5µl of APC-Annexin V, 5 µl of propidium iodide and diluted with 70 µl of binding buffer and incubated in dark at room temperature for 15 minutes. Then the cell suspension was further diluted with binding buffer, transferred to a flat bottom 96-wells plate and applied to flow cytometric analysis. All analyses were performed by a BD FACSArray^{TM} bioanalyser (Becton Dickinson, UK). The instrument was set up to measure the size (forward scatter), granularity (side scatter) and cell fluorescence. Antibody binding was measured by analysing individual cells for fluorescence. The mean fluorescence intensity was determined after correction for cell autofluorescence. Fluorescence histograms were obtained for 10000 individual events. Data was analysed using BD FACSArray^{TM} system software and expressed as a percentage of control fluorescence in arbitrary units.

2.9 Statistical analysis

The statistical significance of the differences between samples was determined using one-way analysis of variance (ANOVA) followed by the posthoc Tukey's test using Minitab software. Differences were considered significant at $p<0.05$.

3. Results and discussion

3.1. The influence of ultrasound on physicochemical properties of HA

The viscosity and GPC results showed that HA with initially high molecular weight (2882±24.50 kDa) was effectively depolymerised even after a relatively short exposure (i.e. 10 minutes) to ultrasound (Table 2). The viscosity of 0.1% w/v solution of native HA was about 17 times higher than the viscosity of water at 25 ºC (Table 2). Ultrasonication resulted in a reduction of the viscosity of HA solution depending on the duration of exposure (Table 2). The decrease in viscosity of HA was very rapid during the first 30 min and decelerated when sonication was maintained for longer times (1-6 hours). Ultrasonic treatment also resulted in the reduction of the molecular weight of HA (Mn and Mw) as a result of depolymerisation (Table 2).

The native HA was heterogeneous in terms of molecular weight distribution and had a high polydispersity of approximately 3.73 (Table 2), however even a short sonication time (10 minutes) caused a significant drop in the polydispersity index (Mw/Mn) leading to an increase in the polymer molecular weight homogeneity. After 30 minutes of sonication the decrease in Mw/Mn values was still noticeable, however with a further increase in the sonication treatment the decrease in heterogeneity of the polymer became less pronounced (Table 2).

Ultrasonication has been reported as a simple and efficient method of obtaining HA of lower molecular weight from the original high molecular weight compound (Lapčík et al., 1998). It is generally accepted that mechanical force is the factor causing depolymerisation of HA during a sonication process. Depolymerisation by ultrasonication depends on the process parameters and it is characterised by a limiting molecular weight (Miyzaki et al., 2001). Indeed, we observed that after 4 and 6 hours of sonication the reduction in the molecular weight, although significant (p-value=0.0014), was less apparent than compared with the first 30 minutes of sonication. Drimalova et al. (2005) reported that prolonged sonication of HA results in a gradual depolymerisation levelled to a limiting molecular weight of 100 kDa. Based on those findings, it can be assumed that applying the current sonication conditions, the molecular weight of 176 kDa for HA obtained after 6 hours of sonication is close to the limiting molecular weight value and a further increase in sonication time would not decrease the molecular weight markedly.

Structural changes in sonicated HA were investigated by H^1NMR, FTIR and UV. H^1NMR showed viscosity dependent intensities of the spectra (data not shown), consistent with the report of Alkrad at el. (2003), however no peak shifts were observed. FTIR spectra of HA, pre- and post- sonication, were very similar indicating no other than molecular weight changes in the polymer structure (Fig. 1A). No shifts of the asymmetric COO^- stretching band at 1616 cm^{-1} nor the amide I vibration at 1653 cm^{-1} (Bezakova et al., 2008) were discerned, however the originally broad and asymmetric absorption at 3100-3600 cm^{-1} assigned to the hydrogen bonding amine and hydroxyl groups of HA appeared to broaden even more when the HA was subjected to sonication. This in contrast to observations of (Bezakova et al., 2008), where narrowing of the H-bond band, assigned to a decrease in hydrogen-bond

strength, was noticed as a result of depolymerisation by microwave irradiation. The increase in strength of H-bonds observed in this work can perhaps be explained by increased entropy of the system resulting from shortening the polymer chains, thus enabling better mutual accessibility of H-bond donor and acceptor groups. UV analysis also suggested minor structural differences when comparing native and sonicated HA, visible as slight differences in slopes of the spectra (data not shown), nevertheless no extra absorption bands appeared suggesting decomposition (Drimalova et al., 2005). Therefore it was concluded that sonication only decreased the molecular weight of HA without introducing structural damage to the polymer.

3.2. HA/chitosan nanoparticles – formation and formulation variables

3.2.1 Impact of HA molecular weight

To examine the influence of the molecular weight of HA on the formation and properties of HA/CS nanoparticles, HA polymers with different molecular weights obtained by the sonication process (see section 3.1) were used. Three different HA/CL113 mass mixing ratios with total polymer content (TPC) of 1 mg/ml were selected based on preliminary studies. The HA/CL113 mass mixing ratio (MMR) of 1 resulted in the formation of positively charged NPs, while ratios of 2.5 and 5 resulted in negatively charged NPs (Fig. 2A). NPs with an MMR of 5 were observed to have generally lower zeta potential values compared to those based on an MMR of 2.5 for all molecular weights of HA studied.

When either native HA (HA2882) or HA sonicated for 10 minutes (HA1161) was used, the formation of NPs was accompanied by the presence of visually large flocs for all three MMRs (Fig. 2B). SEM analysis of the precipitate revealed that those flocs were not composed of discreet nanoparticles or even microparticles, but

358 rather formed a bed of material with a rough surface (Fig. 3a). The amount of
359 precipitating flocs was 26.5±3.0% and 24.2±0.6% of the overall particulates formed
360 when native HA was used to prepare NPs with MMR=5 and MMR=1, respectively,
361 while for HA1161 it was 27.1±10.7% and 29.0±0.5% for MMR=5 and MMR=1,
362 respectively.

363 Formulations with HA sonicated for shorter periods (especially 30 minutes,
364 HA590) were more turbid compared to formulations with HA of lower molecular
365 weights (Fig. 2C). Since the theoretical yields of NPs formed using HA sonicated for
366 different times should be the same, as identical amounts of HA were used, the
367 differences in transmittance may be related to changes in particle size due to the
368 higher molecular weight of HA used. As both HA and chitosan are polymers with
369 high molecular weight, and their solutions in water are viscous, the high viscosity
370 may impair the mixing process and so favour the formation of aggregates (Mackay et
371 al., 2006). The sonication process, and thus the reduction of the molecular weight of
372 HA, renders the solution less viscous (Table 2). The formulation with a HA/CL113
373 MMR of 5 was more transparent than those with MMRs of 2.5 and 1 for the whole
374 range of molecular weights of HA examined.

375 For all the HA/CL113 MMRs tested (5, 2.5 and 1) sonication of HA used for
376 preparation of the NPs for at least 30 minutes resulted in a decrease in the particle size
377 (Fig. 2B) and no aggregation was seen to occur (Fig. 2C). SEM showed well-
378 developed nanostructures (Fig. 3b). No further change in the particle size was
379 observed when HA was sonicated for up to 6 h (HA176). Generally, PDI values (Fig.
380 2D) and zeta potential (Fig. 2A) also decreased with the increase of the duration of
381 sonication of HA. The reduction in the absolute values of zeta potential is more
382 pronounced when HA solutions sonicated for shorter periods were used and this can

be observed in negatively as well as positively charged particles. Since the pH of the formulations was not seen to be affected by the molecular weight of HA and was approximately 5.8 and 4.4 for all negatively and positively charged samples, respectively, variations in zeta potential values could be explained by a limited ability of the polymer chains to mix effectively due to high viscosity, thus forming large entities having different arrangement of polymers on the surface compared with NPs.

When the duration of ultrasound treatment was increased to 30 minutes and more, it was possible to obtain nanoparticles without the tendency to sediment for at least 24 hours. HA with a molecular weight of 257 kDa, obtained by sonication of native HA for 2h, was used in subsequent studies since its molecular weight appeared to provide the optimum balance between the viscosity of HA solution, leading to the production of non-sedimenting NPs, as well as sonication time.

3.2.2 Impact of chitosan molecular weight and type of counterion

Formation of particles of different sizes including large, fast sedimenting flocs and NPs was observed when high molecular weight salts of chitosan were used (CL213 and G213). It appeared that the flocculating structures in both cases were made of NPs (Fig. 3c and d), but the particulates formed by HA/G213 were irregular and formed cauliflower-like assemblies. The samples were allowed to settle overnight to remove aggregated particles and any NPs remaining in the liquid after 24 h were subsequently characterised. CL113 and G113 produced stable NP dispersions with the exception of MMRs corresponding to charge mixing ratios (CMR) of approximately 1 (see Section 3.2.3).

It was noticed that, even after sedimentation of aggregates, transmittance of CL213 NPs was smaller than CL113 NPs, which did not form sedimenting particles

(Fig. 4A). That may suggest that when chitosan with a higher molecular weight was used, more particles were formed. When the polymer chain is longer, there are more amino groups to interact with carboxyl groups of HA leading to precipitation of the interacting polymer chains as nanoparticles or aggregates. The transmittance values were similar when G213 (after sedimentation) and G113 were studied and for cationic G213 NPs the transmittance was lower than for G113 NPs, consistent with reduced concentration of NPs due to removal of particles (Fig. 4B).

Comparing chitosan glutamate and chloride NPs, it was observed that the glutamate NPs were more negatively charged (Fig. 5A). Since the glutamate contains two carboxylic and one amino residues with pKa values of 2.19, 4.25 and 9.67 (Stahl, Wermuth, 2008), respectively, it exists as a negatively charged deprotonated carboxylate at pH above 5. Hence it can be assumed that not only the chitosan chains, but also the counterion can be involved in the formation of NPs and become incorporated into the particulate. The amount of the glutamate counterion entrapped in the NPs was quantified to be 10.35±0.29% w/w for HA/G113 NPs with MMR=1.67 and 12.50±0.38% w/w for HA/G113 NPs with MMR=0.8. A careful selection of the polymer salt is therefore advised.

Even after sedimentation of aggregates, the particle size (Fig. 5B) and polydispersity indices (Fig. 5C) of CL213 and G213 NPs were greater than CL113 and G113 NPs, suggesting unsuitability of polymers with high molecular weight for the manufacture of stable NP carriers.

3.2.3 Impact of polymer mixing ratio

Generally, negatively charged particles (Fig. 5A) were obtained at high HA contents and their sizes at first decreased slightly or did not change significantly with

433 decreasing HA/CS ratio, however when the polymer's MMR was approaching the
434 charge equivalence point ($n^-/n^+=1$), the particle size rapidly increased and large
435 aggregates were formed consistent with a decrease in particle repulsion as the net
436 surface charge decreased. It was impossible to measure the properties of such systems
437 immediately after preparation, thus the sedimenting samples were characterised after
438 standing for 24h and removing the precipitate (data for those samples is presented as
439 filled symbols in Figs. 5A and 5B). With a further decrease in MMR the particles
440 formed had positive zeta potential values (Fig. 5A). A similar tendency as that for the
441 size was observed for PDI values (Fig. 4C); generally they decreased with increasing
442 content of chitosan (but for formulations with high excess of HA the changes are not
443 significant), then reached the minimum just before the inversion of the particle
444 charge, when the charge mixing ratio was close to 1, to increase again with a further
445 increase in the chitosan content.

446 HA and CS are polyelectrolytes which are able to dissociate in aqueous
447 solutions, resulting in charged polymer chains. For HA, the charge is produced upon
448 dissociation of the carboxylic groups in D-glucuronic acid (pKa of 3.23) and the pKa
449 of HA was estimated to be 2.9 (Lapčík et al., 1998). The pKa value of the amino
450 group of CS is approximately 6.5, therefore in acidic media these amino groups
451 undergo protonation and chitosan becomes a polycation. Furthermore, the charge
452 density (number of charged groups per gram of polymer) of chitosan depends also on
453 its deacetylation degree (Boddohi et al., 2008). It is known that when the polymer
454 charge mixing ratio (CMR) is 1, opposite charges are neutralised and aggregation as
455 well as phase separation is expected to occur (Nizri et al., 2004). The MMR values
456 were hence converted into the equivalent CMRs considering the counterion content,
457 the degree of deacetylation for chitosan and environmental pH.

458 Based on experimental values, the CMR corresponding to complete polymer
459 charge neutralisation for HA/CL113, HA/CL213, HA/G113 and HA/G213 were 1.05,
460 1.02, 0.80 and 0.71, respectively, corresponding to MMRs of 1.56, 1.41, 1.02 and
461 0.94, respectively. Thus only the NPs based on chitosan chloride, but not the
462 glutamate salt, had CMRs close to 1. That deviation of CMR from 1 for HA/G is
463 supportive of the proposed above hypothesis that the glutamate residue is in fact
464 incorporated into the particles and does not act as a counterion only. Distinct zones of
465 NP formation and phase separation and aggregation were also determined visually.
466 When a large excess (in terms of CMR) of one of the polymers was used, the sample
467 had an appearance of a solution. With the quantities of polymers approaching the
468 CMR of 1, the systems first became opalescent, then turbid and finally the NPs were
469 seen to aggregate. Visual observations were confirmed by transmittance measurement
470 (Fig. 4A and B). SEM revealed that at CMR=1 the particle size of formed NPs was
471 very broad and microparticles as well as NPs were formed (Fig. 3e).
472 The type of interactions between the NP constituents was investigated by
473 infrared spectroscopy. FTIR spectra of pure HA and CS showed characteristic bands
474 of ionised polymers, as the polymers used to prepare NPs were sodium and chloride
475 salts, respectively. CS spectrum (Fig. 1B) presented bands at 3418 cm^{-1} of –OH and –
476 NH stretching, 1634 cm^{-1} of amide I, 1521 cm^{-1} of $–NH_3^+$, 1414 cm^{-1} of $–CH_2$ bending
477 and 1154 cm^{-1} of antisymmetric C−O−C stretching (Peniche et al., 2007; Lawrie et al.,
478 2007). FTIR spectrum of HA (Fig. 1B) showed peaks at 3407 cm^{-1} of –OH and –NH
479 stretching, 1653 cm^{-1}, 1616 cm^{-1} as well as 1567 cm^{-1} of amide I and $–COO^-$ (as
480 described in section 3.1), 1412 cm^{-1} of $–CH_2$ bending and 1154 cm^{-1} and 1079 cm^{-1} of
481 antisymmetric C−O−C stretching (Denuziere et al., 1996). The infrared spectrum of
482 the 1:1 w/w CS:HA physical mixture (PM) was dominated by the characteristic

483 vibrations of HA (Fig. 1B), however small differences in the position and appearance
484 of some of the absorption bands of PM were seen in comparison to NPs. The latter
485 had a characteristic broad band at 1629 cm^{-1} of amide I and $–COO^-$, while the band at
486 1562 cm^{-1} was shifted and less prominent compared to that of pure HA (Fig. 1B).
487 Therefore it can be concluded that the polymers retained their ionic character in the
488 NPs and that the type of intermolecular interaction is mainly of electrostatic nature.
489 Apart from the formulations with amounts of polymers close to charge
490 neutralisation, all NP dispersions had an absolute value of zeta potential above 30 mV
491 (Fig. 5A), indicating their good physical stability. The dispersions had pH values
492 between 4.2 and 6.1 with lower values corresponding to higher chitosan contents.
493 Fig. 5D shows that the polymer mixing ratio had a considerable influence on
494 the viscosity of NP suspensions and lower viscosity values were measured for lower
495 CMRs. It has been reported that the particulates themselves barely influence the
496 viscosity (Philip et al., 1989). Our results showed that viscosity may be a useful tool
497 for the estimation of non-complexed residual polymer in the system. When one of the
498 polymers is used in excess, there are still molecules of that polymer which do not
499 participate in the formation of NPs or which only weakly interact with the NPs; these
500 polymer molecules are responsible for the increase in viscosity of the continuous
501 phase.
502
503 **3.2.4 Impact of total polymer concentration**
504 Generally, the yield of particles formed was higher for the higher polymer
505 concentration (transmittance measurements in Figure 4A shows that 0.2% w/v
506 formulations are more turbid compared to 0.1% w/v). For anionic NPs, when a high
507 excess of HA was used, the particle size of 0.1 and 0.2% w/v formulations did not

differ significantly, however at an MMR of 1, the 0.1% w/v NPs were significantly smaller compared to the 0.2% w/v formulations (Fig. 5B). All 0.2% w/v samples had moderate PDI values (between 0.2 and 0.5), while for the 0.1% w/v formulations the PDI values were low (below 0.2), which suggests homogenous size distributions (Fig. 5C).

It was observed that when an excess of one of the polymers was used, viscosity of the 0.2% w/v NP dispersion was greater than that of the 0.1% w/v, however the viscosities of NPs with the MMRs of 1-2.5 (corresponding to the CMRs close to 1) were comparable (Fig. 5D).

3.3 TEM of NPs

TEM micrographs show that the particles are approximately spherical, but in some cases deformations can be observed (Fig. 6). When the HA/CL113 mass MMR was 2.5, the particles appeared to be compact and well defined. The NPs with the HA/CL113 MMR of 5 were composed of a relatively dense core surrounded by a less solid and diffused polymer corona making the NPs less spherical in shape. Similar types of morphologies for HA/CS NPs were deduced, but not observed directly, by Boddohi et al., (2009), who noticed that as the charge mixing ratio was farther from 1, the relative size of the polymer corona was increased. Fig. 6A may suggest that the polymer used in insufficient quantity in terms of charge neutralisation is localised mainly in core, while the polymer in excess is present in the core as well as in the corona, being the dominant constituent and responsible for surface charge of the particle.

3.3. Isoelectric points of NPs

Table 3 shows the isoelectric points (IEPs) of selected HA/chitosan NPs. Most of the negatively charged formulations tested (MMRs of 2.5 and 5) had IEPs close to 3. The IEP shifted to more acidic pH values with increasing content of HA in the systems (2.83 for the HA/CL113 MMR of 2.5 and 2.47 for the MMR of 5). When the HA/CL113 mass mixing ratio was 1, the IEP of this formulation was 7. When the total polymer concentration was increased to 0.2% w/v, or when glutamate salt was used instead of chloride, the isoelectric point was not affected (p-value of 0.8678 and 0.9006, respectively). A change in the molecular weight slightly affected the values of IEP, however the differences between the IEPs of nanoparticles composed of 250 kDa HA were not significantly different (p-value of 0.0784 and 0.2864) from either 590 kDa HA or 175 kDa HA. Thus, the HA/CS mass mixing ratio appears to be the most important factor influencing the IEP.

The surface of NPs becomes more negatively charged with increasing pH, and the increase in hydrogen ion concentration leads to an increase in positive charge of the particles. However, aggregation of NPs was observed even when the surface charge of the particles decreased to about ±10 mV.

Depending on the route of administration, NPs may be exposed to different environmental pH values. Thus the IEP (the pH at which a particular molecule or surface carries no net electrical charge) is a very important property of NPs as at a pH near the isoelectric point colloids are usually unstable and flocculation is likely to occur. Thus is appears that the NPs with MMRs of 2.5 and 5 will be stable at physiological pH values of 7.35-7.45, while those with the MMR of 1 should be preferred when used in acidic environments. We found no statistical difference (p-value of 0.0760) in the particle size of the HA/CL113 NPs with an MMR of 2.5 in the pH range of 5.9-7.4 (the size range was 170-215 nm), while the NPs with an MMR of

558 1 remained stable as nanoparticulate dispersions within the pH range of 2-5.9 (the
559 mean NP size was 194-260 nm), whereas at pH of 7.4 the particles flocculated within
560 a few hours.
561
562 **3.4. Stability of HA/CL113 nanoparticles after storage at room temperature**
563 For the evaluation of dispersion stability of NPs upon storage at RT two
564 negatively charged (HA/CL113 the MMRs of 2.5 and 5) and one positively charged
565 formulation were selected (MMR of 1). Fig. 7 shows changes in the particle size, zeta
566 potential and PDI for the two formulations over 28 days storage at RT.
567 Positively charged NPs (MMR of 1) were the least stable formulation. First
568 signs of sedimentation were visually observed after two weeks of storage, while for
569 both formulations containing negatively charged NPs (MMRs of 2.5 and 5) the first
570 signs of sedimentation were noticeable after 3 weeks. After 4 weeks it was possible to
571 observe sediment at the bottom of the vial for all samples, especially for positively
572 charged.
573 The particle size of positively charged NPs decreased systematically from 239
574 (day 0) to 152 nm (day 28) (p-value < 0.0001) (Fig. 7A). A similar trend was
575 observed for PDI, which decreased from the initial value of 0.270 to 0.150 after 28
576 days (p-value < 0.0001) (Fig. 7B). The zeta potential remained steady for 21 days (51-
577 52 mV), and in the fourth week of storage it slightly decreased to 47 mV (Fig. 7C).
578 The samples became more transparent during storage (the transmittance increases
579 from 58% initially to 70% after 3 weeks, data not shown).
580 In contrast, the size of negatively charged NPs with the HA/CL113 MMR of
581 2.5 systematically increased during storage from 188 to 221 nm (p-value = 0.0003)
582 and the PDI values remained low (Fig. 7C). The transmittance values decreases from

583 68% to 54% after 3 weeks (data not shown), so they became more turbid. For both
584 negatively charged formulations the initial value of the zeta potential did not differ
585 significantly (p-value of 0.0938 and 0.7856 for MMR 5 and 2.5, respectively) from
586 the zeta potential value after 4 weeks of storage, and slight fluctuations of zeta
587 potential could be observed (Fig. 7C). Interestingly, there was an initial increase in
588 particle size and polydispersity of the formulation with the HA/CL113 MMR of 5 -
589 the hydrodynamic diameter and PDI reached its peak values after the third day of
590 storage and then decreased to values which did not differ significantly (p-value of
591 0.1692 for size; p-value of 0.4691 for PDI) from the initial values (Fig. 7A and 6B).
592 That increase in the particle size was however minor as the size increased only by
593 about 10% however, it may suggest reorganisation of NPs in the medium.
594
595 **3.5. Cytotoxicity studies**
596 **3.5.1. HA post-sonication**
597 The cytotoxicity of sonicated HA used for the production of the nanoparticles
598 was examined. HA with three molecular weights were tested (590, 257 and 176 kDa
599 obtained by sonication of native HA for 0.5h, 2h and 6h, respectively) at a
600 concentration of 0.5% w/v (which is much higher than the mass of HA in NPs) by
601 MTS assay and flow cytometry (FC). It can be observed from MTS results (Fig. 8A),
602 that the HA samples tested not only exhibited a lack of negative effects on cellular
603 viability, but instead the number of living cells was approximately 10-20% higher
604 than the control. This may suggest that HA either has a cytoprotective effect on cells,
605 or may increase their proliferation rate (Kawasaki et al., 1999). Moreover, the
606 molecular weight of HA did not have an effect on cell viability.

607 The above HA samples were also analysed for apoptotic/necrotic incidence
608 using FC. This assay showed that the viability of control cells and cells treated with
609 all HA samples was comparable (there was no significant difference between any of
610 them, Fig. 8B and 8C), thus it can be stated that sonication did not result in formation
611 of HA with adverse toxicological effects on the cells.
612
613 **3.5.2 Nanoparticles**
614 For the evaluation of NP cytotoxicity, one negatively charged (HA/CL113
615 with an MMR of 5) and one positively charged formulation (with an MMR of 1) were
616 chosen. The zeta potential of NPs with an MMR of 1 in serum-free media (pH=7.4)
617 inverted and was measured to be -17.2±1.25 mV, consistent with the IEP of the
618 formulation of approximately 7. The % of viable Caco-2 cells measured by MTS
619 assay in serum-free media at pH 7.4 for the NP concentrations 20-500 μg/ml and
620 chitosan (CL113) concentrations 125-5000 μg/ml was not significantly different from
621 the control. A change in the colour of medium to orange followed by precipitation
622 was observed upon dissolving chitosan in serum free media. As mentioned earlier, the
623 pKa of amino group of chitosan is 6.5, so at pH 7.4 only about 10% of amino groups
624 of chitosan would be dissociated. Since chitosan is poorly soluble in aqueous
625 solutions with neutral or basic pH (Kudsiova, Lawrence, 2008), the concentration of
626 chitosan remaining in solution will be much smaller due to precipitation of non-
627 ionised chitosan chains. That may explain why the viability of Caco-2 cells is not
628 affected by chitosan at pH 7.4. Also, it has been shown that the degree of chitosan
629 toxicity depends on the charge density, configurational arrangements of the cationic
630 residues and degree of deacetylation (Kudsiova, Lawrence, 2008; Schipper et al.,
631 1996). Also, Loretz et al. (2007) reported that the zeta potential is the key feature that

632 contributes most to the toxicity of chitosan NPs, while the size of the particles only
633 slightly affects their toxicity.

634 Considering the impact of pH on the toxicity of NPs formulations, serum free
635 media without sodium bicarbonate (pH 5.0) was also used for the MTS experiments.
636 The zeta potential values for the HA/CL113 formulations measured in this modified
637 medium were 20.3±0.314 and -18.7±0.247 mV for NPs with MMR=1 and MMR=5,
638 respectively. A concentration-dependent cytotoxicity was observed for chitosan on its
639 own (CL113) and NPs with MMR=1 (Fig. 9). The IC_{50} values calculated from the cell
640 viability-concentration graph were significantly different (p-value < 0.0001) for the
641 chitosan solutions and NPs with MMR=1 and were 25.9±1.02 μg/ml for chitosan and
642 83.9±2.66 μg/ml for the NPs. Thus, by formulating CL113 as HA-based NPs, the IC_{50}
643 was increased by over 3-fold. This suggests that positively charged HA/CL113 NPs
644 can be used as a less toxic alternative to chitosan formulations. HA/CL113 with
645 MMR=5 were found be non-toxic in the whole range of concentration studied and
646 furthermore, cytoprotective effects were seen, similar to those when HA on its own
647 was used as described above, at higher HA concentrations (Fig. 9). It can be
648 concluded that HA present in the NPs seems to play a protective role neutralising the
649 toxic effects of chitosan.
650

651 **4. Conclusions**

652 A production method aimed at fabrication of novel, cross linker-free and non-
653 sedimenting NPs was successfully developed. The physicochemical properties of the
654 NPs were found to be conveniently adjusted by changing the formulation conditions:
655 polymer mixing ratio, total polymer concentration, the molecular weight of the
656 polymers and the type of the counterion in the chitosan salt. The main factor

determining particle formation and properties was the mixing ratio of the polymers. However, other parameters, e.g. the salt of chitosan used and the total polymer concentration also played a role. The influence of molecular weight of the polymer was especially pronounced in the range of higher molecular weights. A change in HA/CS mass ratio considerably changed the physicochemical properties of the nanoparticles, especially the zeta potential. A decrease in the HA content was accompanied by an increase in zeta potential and its inversion from negative to positive values. Fine-tuning of the HA/CS ratio allowed for non-toxic NPs at pH=5 and 7.4 to be produced, a vital property when NPs are formulated for e.g. the oral route of administration.

Overall, the HA/CS NPs obtained can be considered as viable and non-toxic carriers for formulating bioactive compounds due to their favourable physicochemical and biopharmaceutical properties.

Acknowledgment

This study was funded by the Irish Drug Delivery Research Network, a Strategic Research Cluster grant (07/SRC/B1154) under the National Development Plan co-funded by EU Structural Funds and Science Foundation Ireland. CM is SFI Stokes lecturer. KJP is funded by the Solid State Pharmaceutical Cluster, supported by Science Foundation Ireland under grant number 07/SRC/B1158. The authors are grateful to Dr. Deirdre D'Arcy for her help in correcting this manuscript and useful discussions.

References:

Afzal, A., Afzal, M., Jones, A., Armstrong, D., 2002. Rapid determination of glutamate using HPLC technology. Meth. Mol. Biol. 186, 111-115.

Agnihotri, S.A., Mallikarjuna, N.N., Aminabhavi, T.M., 2004. Recent advances on chitosan-based micro- and nanoparticles in drug delivery. J. Control. Release 100, 5-28.

Alkrad, J.A., Mrestani, Y., Stroehl, D., Wartewig, S., Neubert, R., 2003. Characterization of enzymatically digested hyaluronic acid using NMR, Raman, IR, and UV-Vis spectroscopies. J. Pharm. Biomed. Anal. 31, 545-550.

Bezakova, Z., Hermannova, M., Drimalova, E. , Malovikova, A., Ebringerova, A. , Velebny, V., 2008. Effect of microwave irradiation on the molecular and structural properties of hyaluronan. Carbohydr. Polym. 73, 640-646.

Boddohi, S., Moore, N., Johnson, P., Kipper, M., 2009. Polysaccharide-based polyelectrolyte complex nanoparticles from chitosan, heparin, and hyaluronan. Biomacromolecules 10, 1402-1409.

Boryniec, S., Strobin, G., Struszczyk, H., Niekraszewicz, A., Kucharska, M., 1997. GPC studies of chitosan degradation. Int. J. Polym. Anal. Charact. 3, 359-368.

Choi, K.Y., Chung, H., Min, K.H., Yoon, H.Y., Kim, K., Park, J.H., Kwon, I.C., Jeong, S.Y., 2010. Self assembled hyaluronic acid nanoparticles for active tumor targeting. Biomaterials 31, 106-114.

de la Fuente, M., Seijo, B., Alonso, M.J., 2008a. Novel hyaluronic acid-chitosan nanoparticles for ocular gene therapy. Invest. Ophthalmol. Vis. Sci. 49, 2016-2024.

de la Fuente, M., Seijo, B., Alonso, M.J., 2008b. Design of novel polysaccharidic nanostructures for gene delivery. Nanotechnol. 19, 075105-075114.

705 Denuziere, A., Ferrier, D., Domard, A., 1996. Chitosan-chondroitin sulfate
706 and chitosan-hyaluronate polyelectrolyte complexes. Physico-chemical aspects.
707 Carbohydr. Polym. 29, 317-323.
708 Drimalova, E., Velebny, V., Sasinkova, V., Hromadkova, Z., Ebringerova, A.,
709 2005. Degradation of hyaluronan by ultrasonication in comparison to microwave and
710 conventional heating. Carbohydr. Polym. 61, 420-426.
711 Emerich, D.F., Thanos, C.G., 2003. Nanotechnology and medicine. Expert
712 Opin. Biol. Ther. 3, 655-663.
713 Hirai, A., Odani, H., Nakajima, A., 1991. Determination of degree of
714 deacetylation of chitosan by ^{1}H NMR spectroscopy. Polymer Bulletin 26, 26: 87-94.
715 ICH guideline Q8(R2) "Pharmaceutical development", August 2009
716 Janes, K.A., Calvo, P., Alonso, M.J., 2001. Polysaccharide colloidal particles
717 as delivery systems for macromolecules. Adv. Drug Del. Rev. 47, 83-97.
718 Kaszuba, M., McKnight, D., Connah, M.T., McNeil-Watson, F.K.,
719 Nobbmann, U., 2008. Measuring sub nanometre sizes using dynamic light scattering.
720 J. Nanopart. Res. 10, 823–829.
721 Kawasaki, K., Ochi, M., Uchio, Y., Adachi, N., Matsusaki, M., 1999.
722 Hyaluronic acid enhances proliferation and chondroitin sulfate synthesis in cultured
723 chondrocytes embedded in collagen gels. J. Cell. Physiol. 179, 142-148.
724 Kudsiova, L., Lawrence, M.J., 2008. A comparison of the effect of chitosan
725 and chitosan-coated vesicles on monolayer integrity and permeability across Caco-2
726 and 16HBE14o-cells. J. Pharm. Sci. 97, 3998-4010.
727 Lapčík L. Jr., Lapčík, L., de Smedt, S., Demeester, J., Chabreček, P., 1998.
728 Hyaluronan: preparation, structure, properties and applications. Chem. Rev. 98, 2664-
729 2683.

730 Lawrie, G., Keen, I., Drew, B., Chandler-Temple, A., Rintoul, L., Fredericks,
731 P., Grøndahl, L., 2007. Interactions between alginate and chitosan biopolymers
732 characterized using FTIR and XPS. Biomacromolecules. 8, 2533-2541.
733 Liu, Z., Yanpeng, J., Wang, Y., Zhou, C., Zhang, Z., 2008. Polysaccharide-
734 based nanoparticles as drug delivery systems. Adv. Drug Del. Rev. 60, 1650-1662.
735 Loretz, B., Bernkop-Schnürch, A. , 2007. In vitro cytotoxicity testing of non-
736 thiolated and thiolated chitosan nanoparticles for oral gene delivery, Nanotoxicology
737 1, 139-148.
738 Mackay, M.E., Tuteja, A., Duxbury, P.M., Hawker, C.J., van Horn, B., Guan,
739 Z., Chen, G., Krishnan, R.S., 2006. General strategies for nanoparticle dispersion,
740 Science 311, 1740-1743.
741 Miyazaki, T., Yomota, C., Okada, S., 2001. Ultrasonic depolymerization of
742 hyaluronic acid. Polym. Degrad. Stab. 74, 77-85.
743 Nizri, G., Magdassi, S., Schmidt, J., Cohen, Y., Talmon, Y., 2004.
744 Microstructural characterization of micro- and nanoparticles formed by polymer-
745 surfactant interactions. Langmuir 20, 4380-4385.
746 Oyarzun-Ampuero, F.A., Brea, J., Loza, M.I., Torres, D., Alonso, M.J., 2009.
747 Chitosan-hyaluronic acid nanoparticles loaded with heparin for the treatment of
748 asthma. Int. J. Pharm. 381, 122-129.
749 Paluch, K.J., Tajber, L., McCabe, T., O'Brien, J.E., Corrigan, O.I., Healy,
750 A.M., 2010. Preparation and solid state characterisation of chlorothiazide sodium
751 intermolecular self-assembly suprastructure. Eur. J. Pharm. Sci. 41, 603-611.
752 Parojčić, J., Stojković, A., Tajber, L., Grbić, S., Paluch, K.J., Djurić, Z.,
753 Corrigan, O.I., 2011. Biopharmaceutical characterization of ciprofloxacin HCl-ferrous
754 sulfate interaction. J. Pharm. Sci. 100, 5174-5184.

755 Peniche, C., Fernández, M., Rodríguez, G., Parra, J., Jimenez, J., Bravo, A.L.,
756 Gómez, D., San Román, J., 2007. Cell supports of chitosan/hyaluronic acid and
757 chondroitin sulphate systems. Morphology and biological behaviour, J. Mater. Sci.
758 Mater. Med., 18, 1719-1726.
759 Philipp, B., Dautzenberg, H., Linow, K.J., Kötz, J., Dawydoff, W., 1989.
760 Polyelectrolyte complexes- recent developments and open problems, Prog. Polym.
761 Sci. 14, 91-172.
762 Radziwon-Balicka, A., Medina, C., O'Driscoll, L., Treumann, A., Bazou, D.,
763 Inkielewicz-Stepniak, I., Radomski, A., Jow, H., Radomski, M.W., 2012. Platelets
764 increase survival of adenocarcinoma cells challenged with anticancer drugs:
765 mechanisms and implications for chemoresistance. Br. J. Pharmacol.; doi:
766 10.1111/j.1476-5381.2012.01991.x
767 Schipper, N.G., Vårum, K.M., Artursson, P., 1996. Chitosans as absorption
768 enhancers for poorly absorbable drugs. 1: Influence of molecular weight and degree
769 of acetylation on drug transport across human intestinal epithelial (Caco-2) cells.
770 Pharm. Res. 13, 1686-1692.
771 Stahl, P.H., Wermuth, C.G., 2008, Handbook of pharmaceutical salts
772 properties, selection and use. Wiley-VCH.
773 Stern, R., Asari, A.A., Sugahara, K.N., 2006. Hyaluronan fragments: an
774 information reach system. Eur. J. Cell Biol.85, 699-715.
775 Tajber, L., Corrigan, D.O., Corrigan, O.I, Healy, A.M., 2009. Spray drying of
776 budesonide, formoterol fumarate and their composites--I. Physicochemical
777 characterisation. Int. J. Pharm. 367, 79-85.
778 Varian, Inc. PL aquagel-OH Mixed Data Sheet
779 http://www.varianinc.com/image/vimage/docs/products/consum/gpc-

780 sec/gpcseccolumns/aqueous/shared/pl_aquagel-oh_mixed_ds.pdf accessed on
781 09/05/2012

782 Wadhwa, S., Paliwal, R., Paliwal, S.R., Vyas, S.P., 2009. Hyaluronic acid
783 modified chitosan nanoparticles for effective management of glaucoma: development,
784 characterization, and evaluation. J.Drug Targeting 18, 292-302.

Table 1 Physicochemical characteristics of chitosan salts and native HA used in the studies. DD – degree of deacetylation according to manufacturer's data, DD NMR - degree of deacetylation calculated from nuclear magnetic resonance data, Mn - number average molecular weight, Mw - weight average molecular weight

Polymer	Counter ion	Counter ion content	DD	DD NMR	Mn [kDa]	Mw [kDa]	Mw/Mn
HA	Na^+	3.6%	N/A	N/A	772±9.77	2882±24.50	3.73±0.064
CL113	Cl^-	15.5%	83%	83.5%	33 ±7.33	110±6.78	3.38±0.544
CL213	Cl^-	14.0%	86%	79.8%	113±1.81	340±13.62	3.01±0.169
G113	glutamate	30.6±3.08%	86%	N/A	35±1.93	115±14.16	3.27±0.224
G213	glutamate	30.4±2.94%	86%	N/A	227±21.90	398±37.29	1.75±0.004

Table 2 Physicochemical parameters of native and sonicated HA. Symbols as in Table 1.

Sonication time of HA [hrs]	Sample name	Dynamic viscosity [mPa*s]	Mn [kDa]	Mw [kDa]	Mw/Mn
0	HA2882	15.49±0.815	772±9.77	2882±24.50	3.73±0.064
0.17	HA1161	8.33±0.434	409±9.45	1161±35.99	2.84±0.125
0.5	HA590	4.13±0.225	238±9.45	590±20.44	2.43±0.043
1	HA343	2.91±0.179	145±6.93	343±14.40	2.36±0.044
1.5	HA292	2.37±0.133	128±4.89	292±6.68	2.28±0.039
2	HA257	2.14±0.162	118±4.89	257±8.43	2.18±0.042
4	HA201	1.72±0.025	96±2.51	201±3.40	2.08±0.019
6	HA176	1.49±0.233	86±1.09	176±4.32	2.05±0.028

Table 3 Isoelectric points of HA/CS nanoparticles. TPC – total polymer concentration.

HA type	Type of CS salt	TPC (%)	HA/CS mass mixing ratio	Isoelectric point
HA590	CL113	0.1	2.5	3.76±0.57
HA257	CL113	0.1	2.5	2.83±0.38
HA176	CL113	0.1	2.5	3.10±0.02
HA257	CL113	0.1	1	6.98±0.54
HA257	CL113	0.1	5	2.47±0.25
HA257	G113	0.1	2.5	2.87±0.09
HA257	CL113	0.2	2.5	2.86±0.09

Figure captions

Figure 1. A) FTIR spectra of a) native HA and HA sonicated for b) 2h and c) 6h. B) FTIR spectra of a) CL113, b) HA257, c) 1:1 w/w physical mixture of CL113 and HA257 and d) HA257/CL113 NPs (1:1 w/w).

Figure 2. A) Zeta potential B) Particle size, C), Transmittance and D) Polydispersity of NPs formulated with HA sonicated for various time periods and CL113. TPC was 0.1% w/v. Circles – HA/CL113 with MMR of 5, squares - HA/CL113 with MMR of 2.5 and triangles - HA/CL113 with MMR of 1. Filled symbols indicate flocculating and sedimenting samples, while empty symbols indicate neat NP dispersions.

Figure 3. Scanning electron micrographs of: a) HA2882/CL113 MMR=2.5, b) HA257/CL113 MMR=2.5, c) HA257/CL213 MMR=2.5, d) HA257/G213 MMR=2.5 and e) HA257/CL113 MMR=1.7 (CMR=1). TPC of 0.1% w/v was used in all cases.

Figure 4. Transmittance of A) HA/CS chloride and B) HA/CS glutamate NP systems. HA molecular weight was 257 kDa. Squares – HA/CL113 with TPC of 0.2% w/v, circles - HA/CL113 with TPC of 0.1% w/v, upward triangles - HA/CL213 with TPC of 0.1% w/v, downward triangles - HA/G113 with TPC of 0.1% w/v and diamonds - HA/G213 with TPC of 0.1%. All lines are for visual guidance only. Filled symbols indicate data for flocculating and sedimenting samples obtained after standing samples for 24 h, while empty symbols indicate data obtained immediately after preparing the dispersions. Small empty symbols indicate visually opalescent NP dispersions and large empty symbols indicate dispersions visually transparent. Inset in 4B is for clarity purposes.

Figure 5. A) Zeta potential B) Size, C) Polydispersity and D) Viscosity of various HA/CS NP systems. HA molecular weight was 257 kDa. Squares – HA/CL113 with total polymer concentration (TPC) of 0.2% w/v, circles - HA/CL113 with TPC of 0.1% w/v, upward triangles - HA/CL213 with TPC of 0.1% w/v, downward triangles - HA/G113 with TPC of 0.1% w/v and diamonds - HA/G213 with TPC of 0.1% w/v. All lines are for visual guidance only. Filled symbols indicate data for flocculating and sedimenting samples obtained after standing samples for 24 h, while empty symbols indicate data obtained immediately after preparing the dispersions.

Figure 6. TEM micrographs of HA/CL113 NPs with MMR of A) 5 and B) 2.5. HA molecular weight was 257 kDa and TPC was 0.1% w/v.

Figure 7. Stability studies of NPs dispersions at room temperature: A) particle size, B) polydispersity and C) zeta potential. Triangles - HA/CL113 NPs with MMR of 1, circles - HA/CL113 NPs with MMR of 2.5 and squares - HA/CL113 NPs with MMR of 5. HA molecular weight was 257 kDa and the total polymer concentration was 0.1% w/v. All lines are for visual guidance only.

Figure 8. A) Cell viability (MTS assay, empty bars) and apoptosis (flow cytometry, hashed bars) in Caco-2 cells after 72 h treatment with HA 0.5% w/v solutions of the polymer with molecular weight of 590, 257 and 176 kDa. B) C) and D) Scatter plots for apoptosis assay – control, HA with molecular weight of 590 and 176 kDa, respectively. HA sonicated induced similar apoptosis/necrosis events in Caco-2 cells compared to the control. Representative recordings of 3 similar experiments. Q1:

necrotic cell zone, Q2: late apoptosis or dead cell zone Q3: living cell zone Q4: viable apoptotic cell zone.

Figure 9. Cell viability (MTS assay) for Caco-2 cells as a function of chitosan concentration. Squares indicate chitosan (CL113), triangles HA/CL113 NPs with MMR of 1 and circles HA/CL113 NPs with MMR of 5. The treatment time was 24 h using medium at pH=5.0. The dashed line indicates 50% cell viability. Viability of the control group was 100% (dotted line).

Figures in colour for on-line version

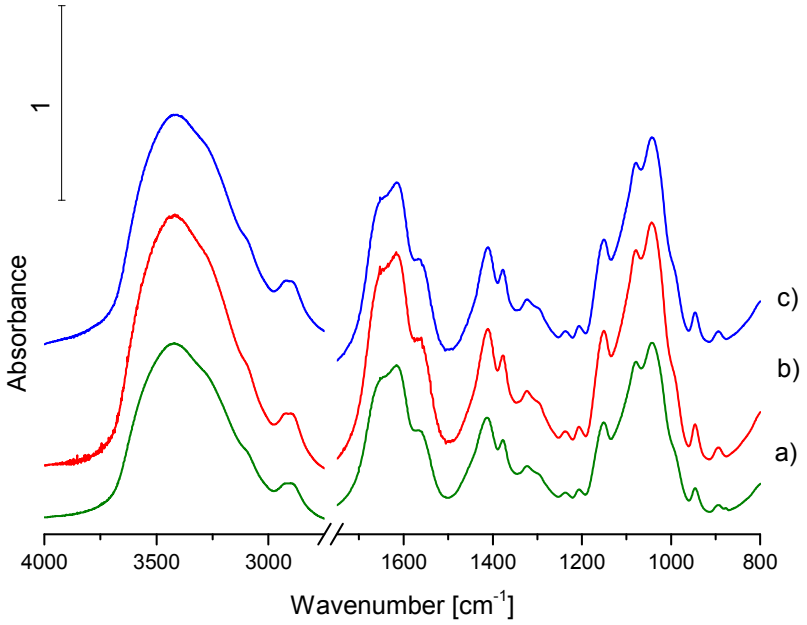

Fig. 1A

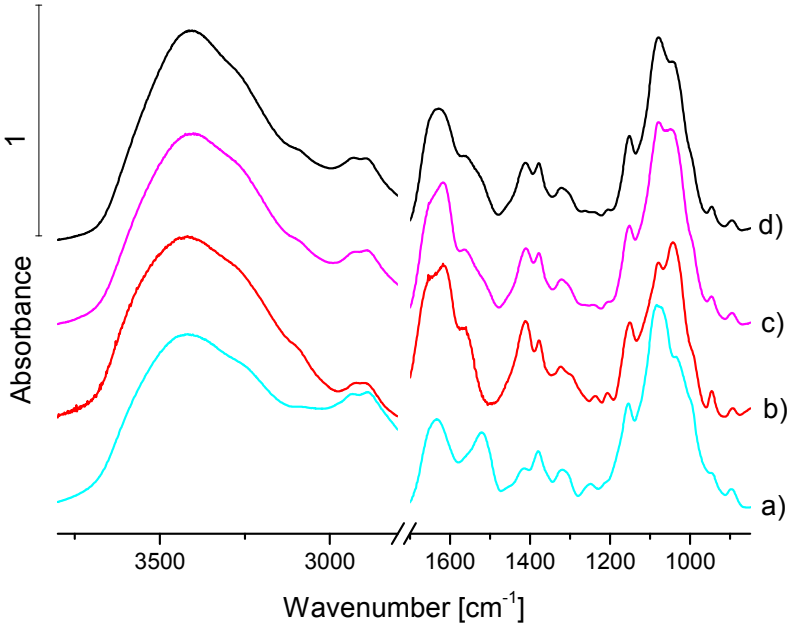

Fig. 1B

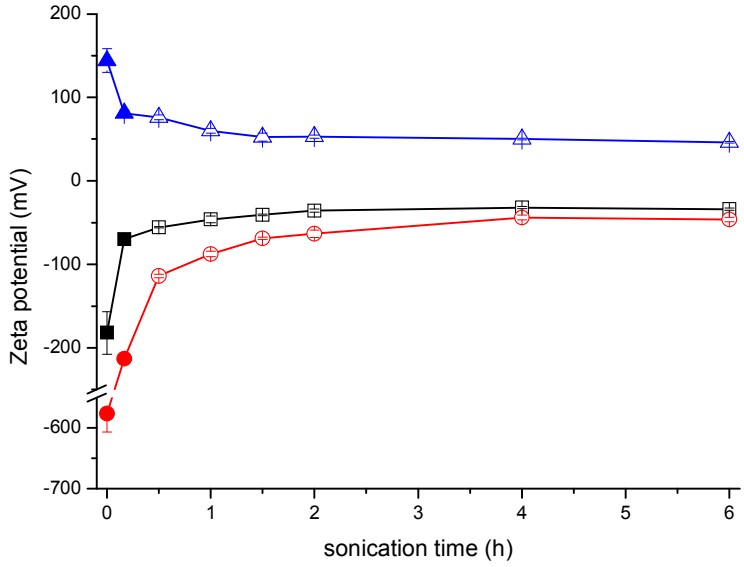
Zeta potential (mV)
200
100
0
-100
-200
-600
-700
0
1
2
3
4
5
6
sonication time (h)

Fig. 2A

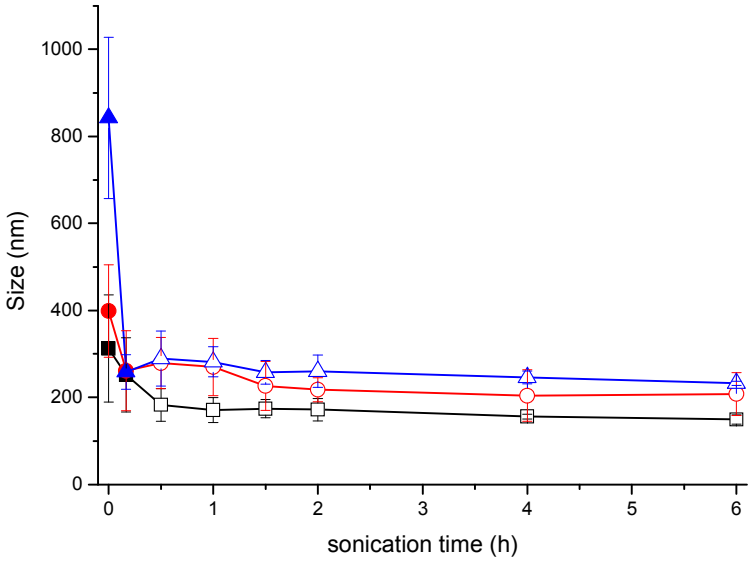
Size (nm)
1000
800
600
400
200
0
0
1
2
3
4
5
6
sonication time (h)

Fig. 2B

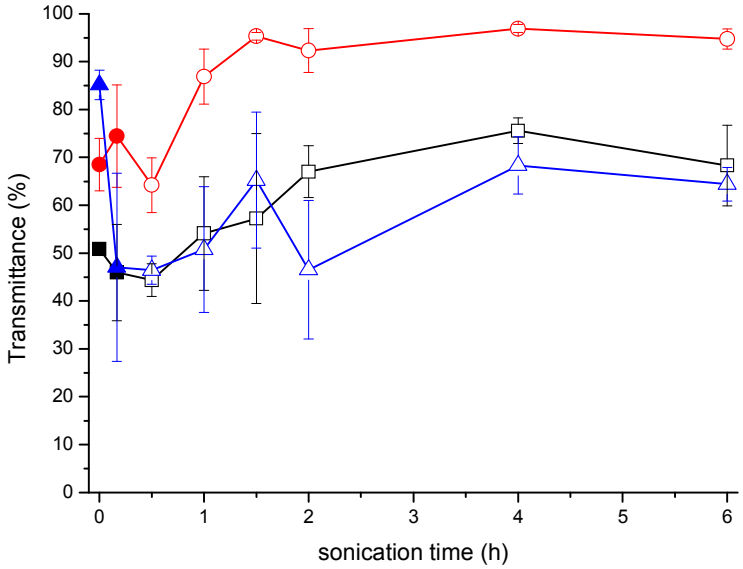
Transmittance (%)
sonication time (h)
100
90
80
70
60
50
40
30
20
10
0
0
1
2
3
4
5
6

Fig. 2C

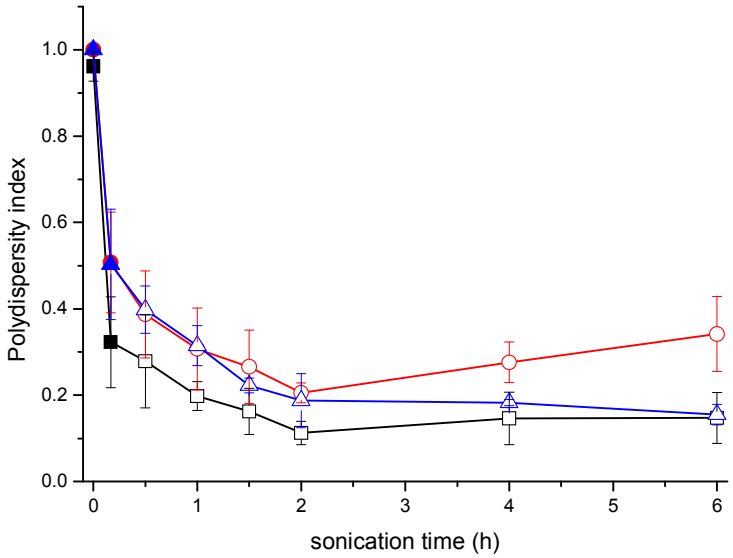
Polydispersity index
sonication time (h)
1.0
0.8
0.6
0.4
0.2
0.0
0
1
2
3
4
5
6

Fig. 2D

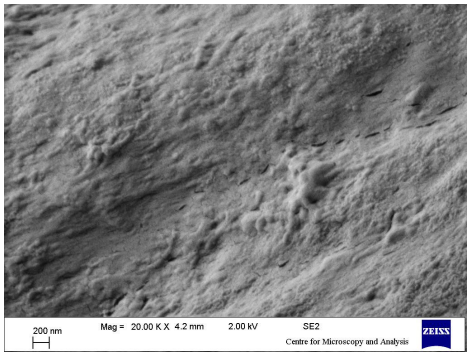
200 nm
Mag = 20.00 K X 4.2 mm
2.00 kV
SE2
Centre for Microscopy and Analysis
ZEISS
a)
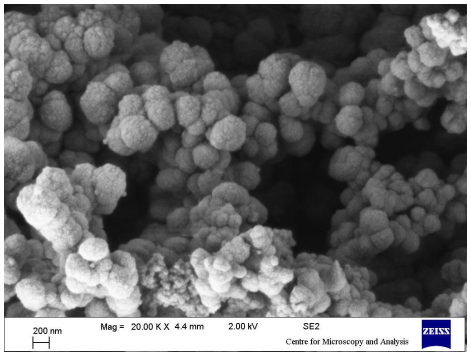
200 nm
Mag = 20.00 K X 4.4 mm
2.00 kV
SE2
Centre for Microscopy and Analysis
ZEISS
b)
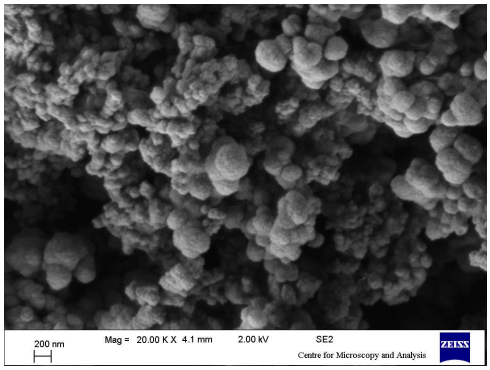
200 nm
Mag = 20.00 K X 4.1 mm
2.00 kV
SE2
Centre for Microscopy and Analysis
ZEISS
c)
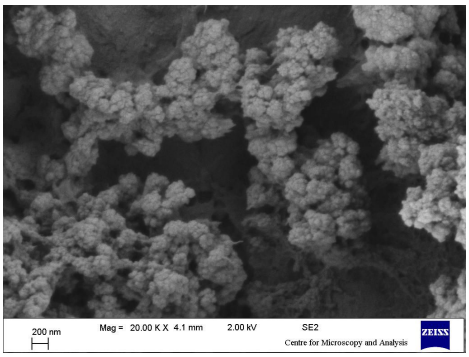
200 nm
Mag = 20.00 K X 4.1 mm
2.00 kV
SE2
Centre for Microscopy and Analysis
ZEISS
d)
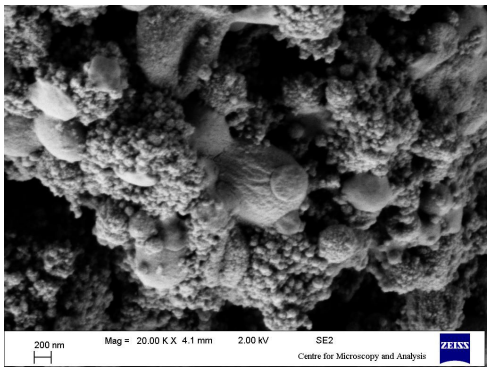
200 nm
Mag = 20.00 K X 4.1 mm
2.00 kV
SE2
Centre for Microscopy and Analysis
ZEISS
e)

Fig. 3

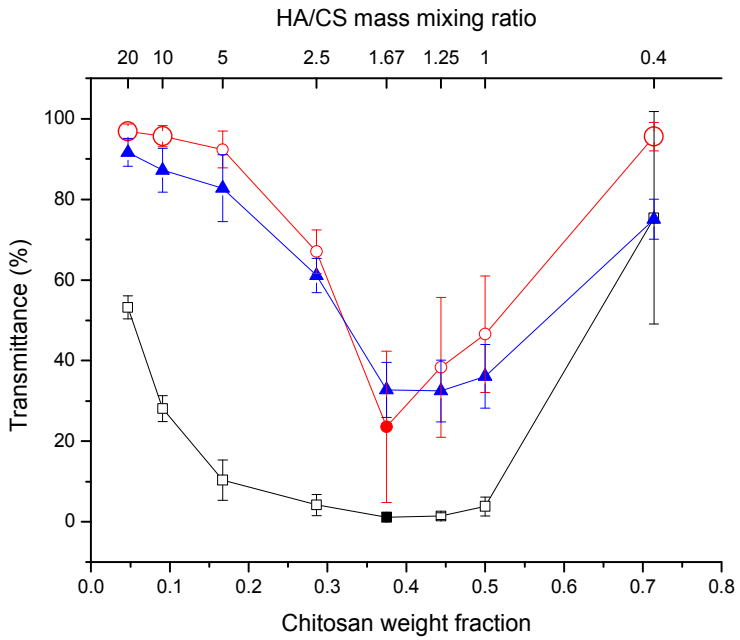
HA/CS mass mixing ratio
20 10 5 2.5 1.67 1.25 1 0.4
Transmittance (%)
Chitosan weight fraction

Fig. 4A

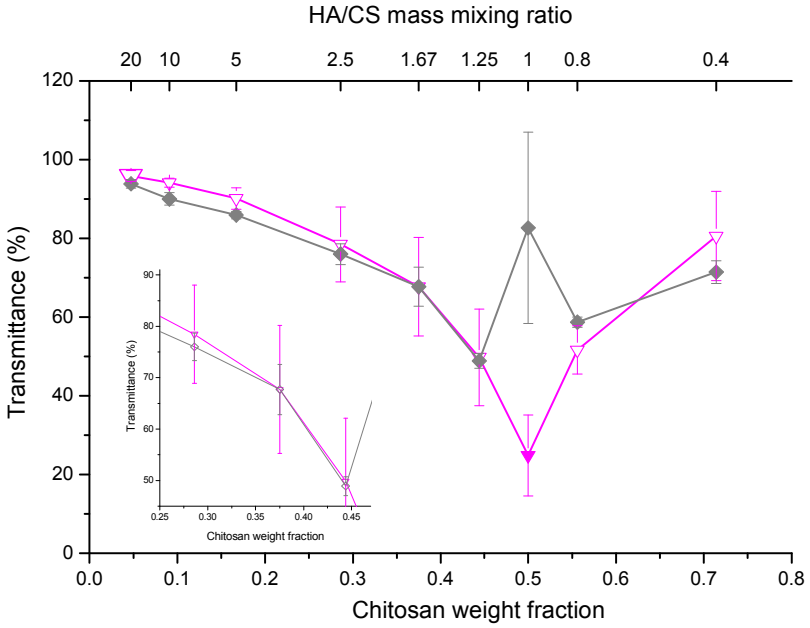
HA/CS mass mixing ratio
20 10 5 2.5 1.67 1.25 1 0.8 0.4
Transmittance (%)
Chitosan weight fraction
Transmittance (%)
Chitosan weight fraction

Fig. 4B

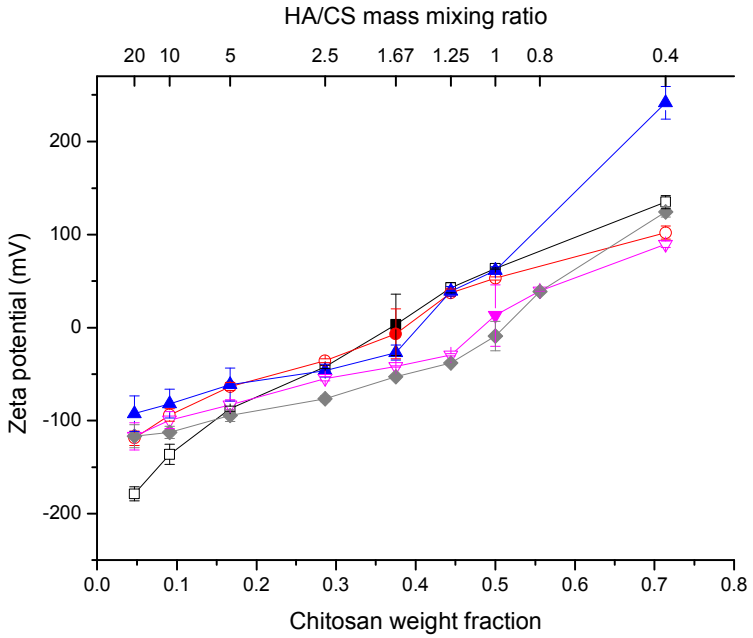
HA/CS mass mixing ratio
20
10
5
2.5
1.67
1.25
1
0.8
0.4
Zeta potential (mV)
200
100
0
-100
-200
0.0
0.1
0.2
0.3
0.4
0.5
0.6
0.7
0.8
Chitosan weight fraction

Fig. 5A

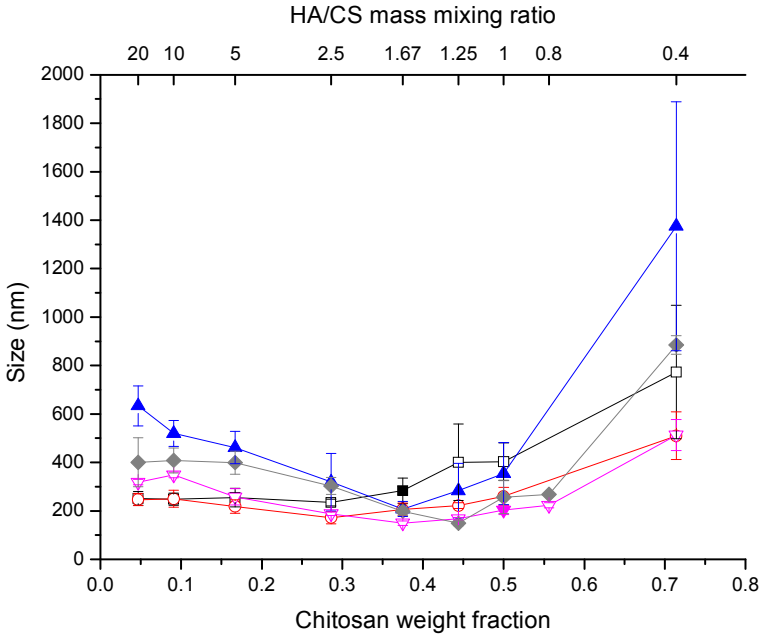
HA/CS mass mixing ratio
20
10
5
2.5
1.67
1.25
1
0.8
0.4
Size (nm)
2000
1800
1600
1400
1200
1000
800
600
400
200
0
0.0
0.1
0.2
0.3
0.4
0.5
0.6
0.7
0.8
Chitosan weight fraction

Fig. 5B

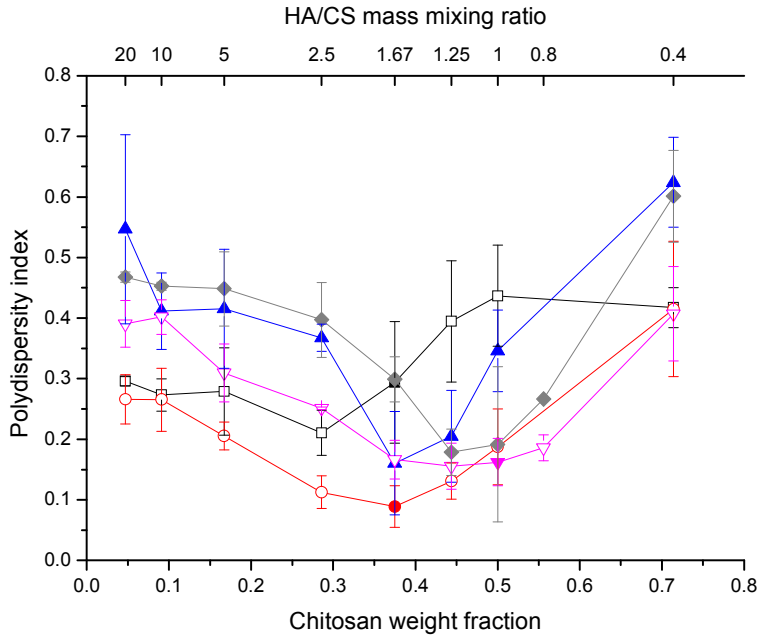
HA/CS mass mixing ratio
20 10 5 2.5 1.67 1.25 1 0.8 0.4
Polydispersity index
0.0 0.1 0.2 0.3 0.4 0.5 0.6 0.7 0.8
Chitosan weight fraction

Fig. 5C

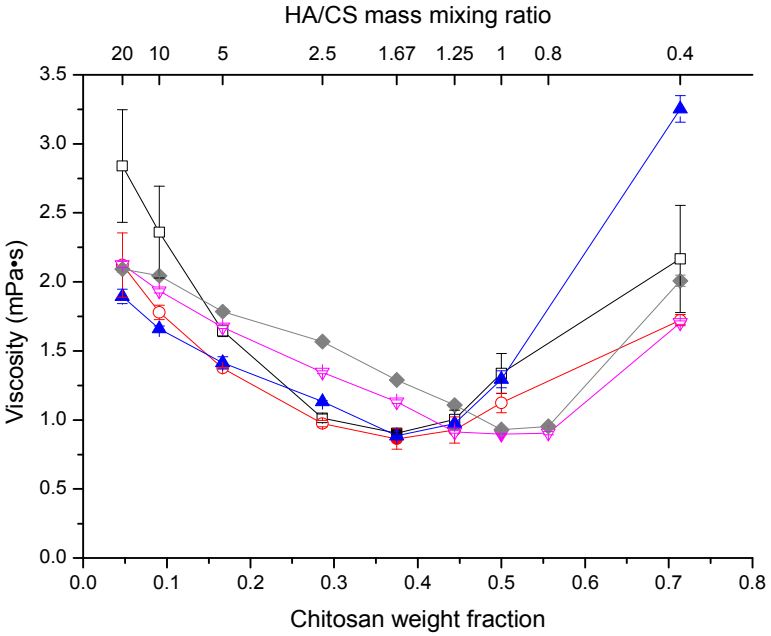
HA/CS mass mixing ratio
20 10 5 2.5 1.67 1.25 1 0.8 0.4
Viscosity (mPa•s)
0.0 0.5 1.0 1.5 2.0 2.5 3.0 3.5
0.0 0.1 0.2 0.3 0.4 0.5 0.6 0.7 0.8
Chitosan weight fraction

Fig. 5D

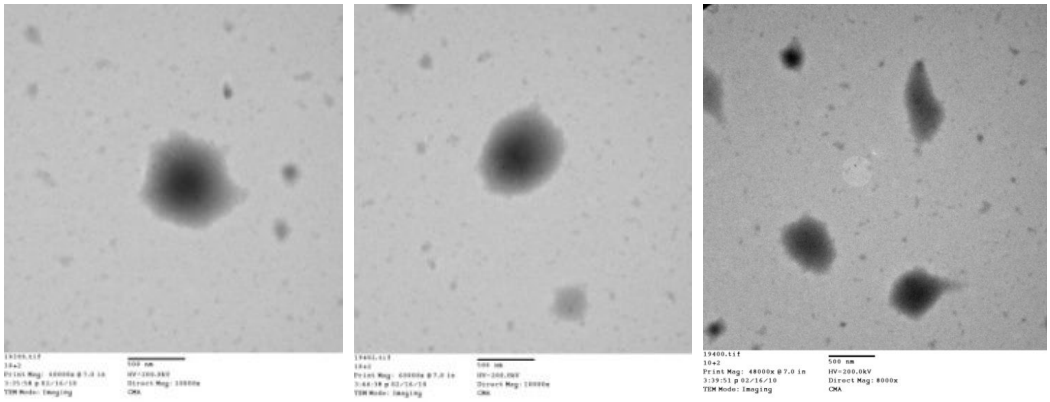

A)

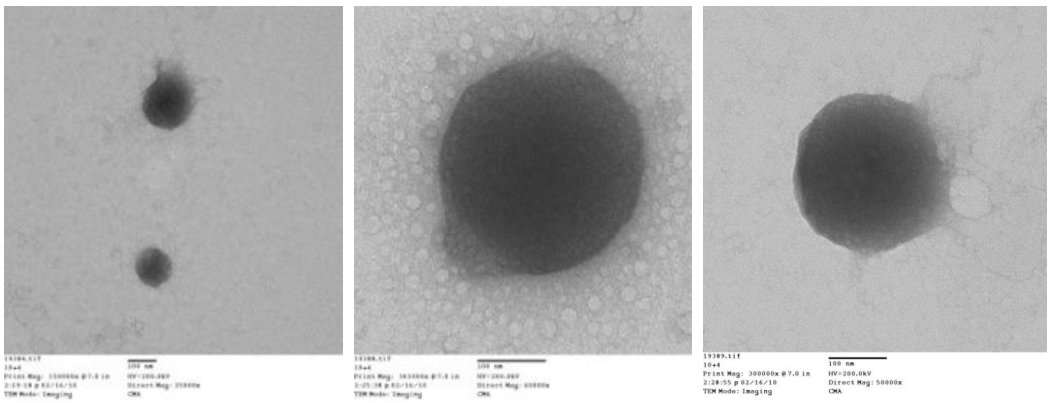

B)

Fig. 6

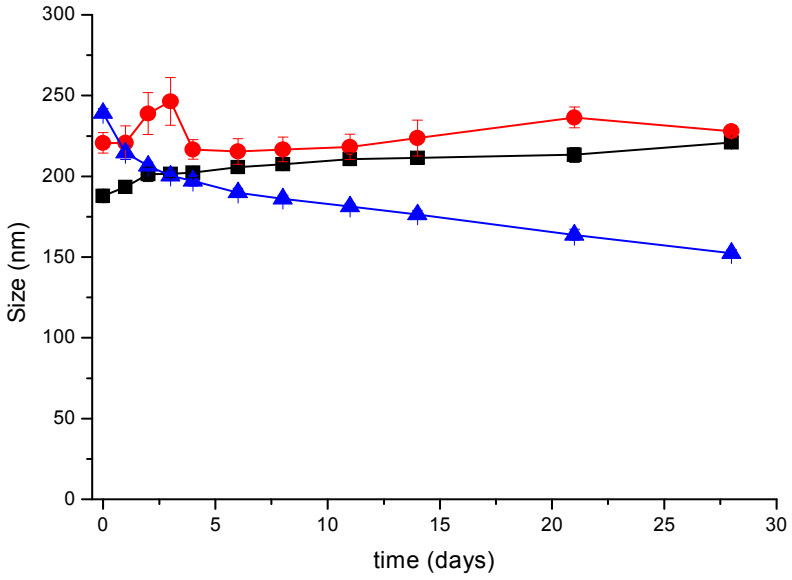
Size (nm)
time (days)
300
250
200
150
100
50
0
0
5
10
15
20
25
30

Fig. 7A

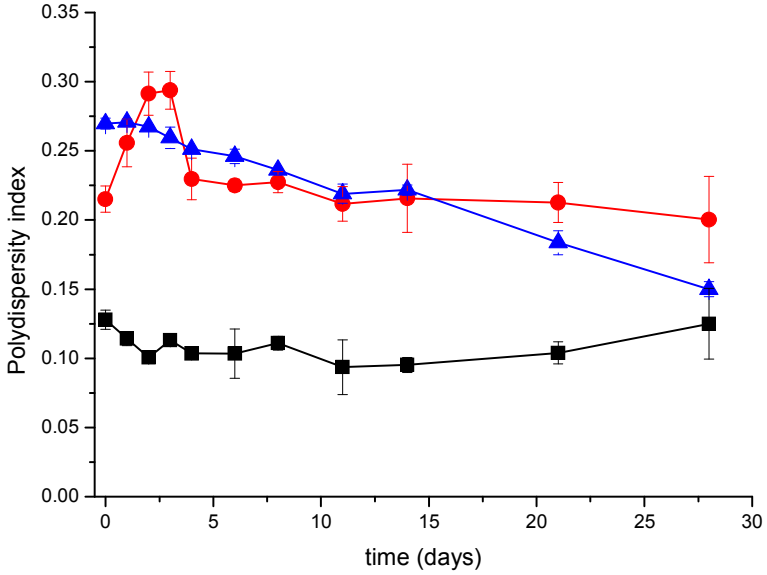
Polydispersity index
time (days)
0.35
0.30
0.25
0.20
0.15
0.10
0.05
0.00
0
5
10
15
20
25
30

Fig. 7B

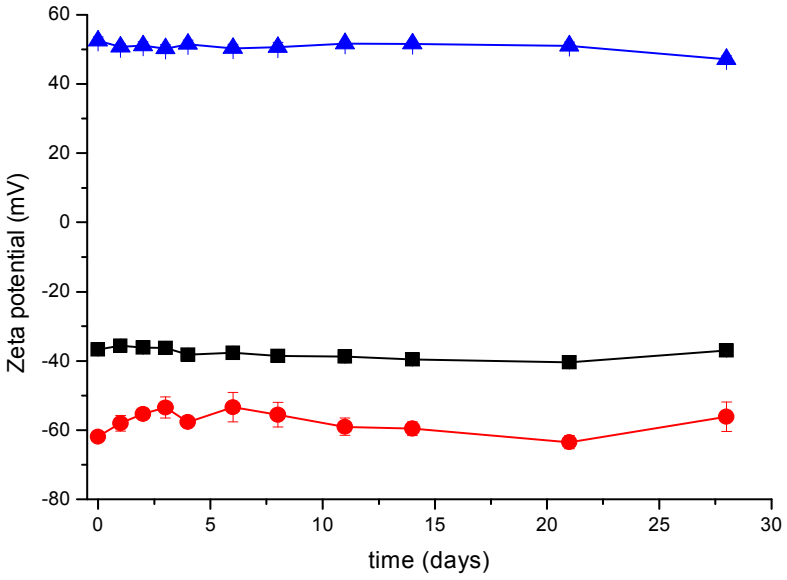
60
40
20
0
-20
-40
-60
-80
Zeta potential (mV)
0
5
10
15
20
25
30
time (days)

Fig. 7C

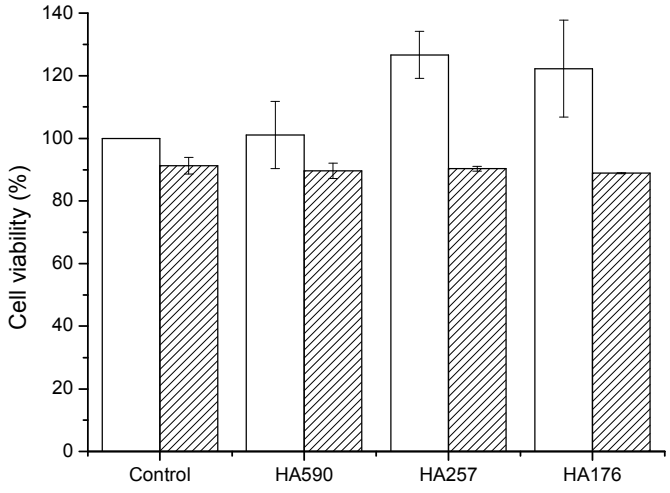

Fig. 8A

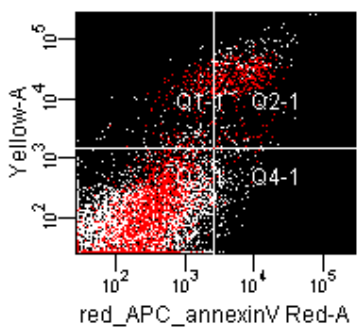

B)

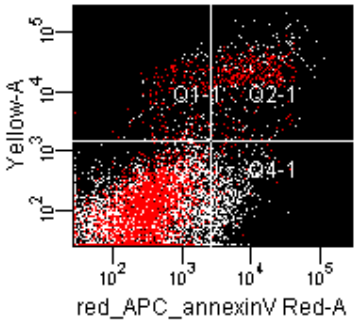

C)

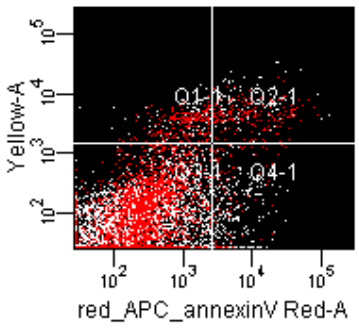

D)

Fig. 8BCD

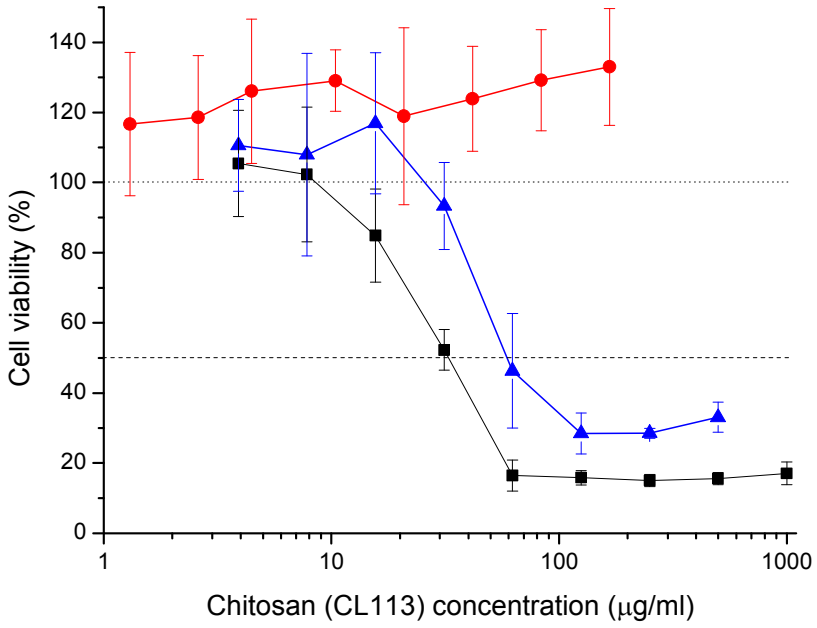
Cell viability (%)
140
120
100
80
60
40
20
0
1
10
100
1000
Chitosan (CL113) concentration (μg/ml)

Fig. 9

Black&white versions of figures

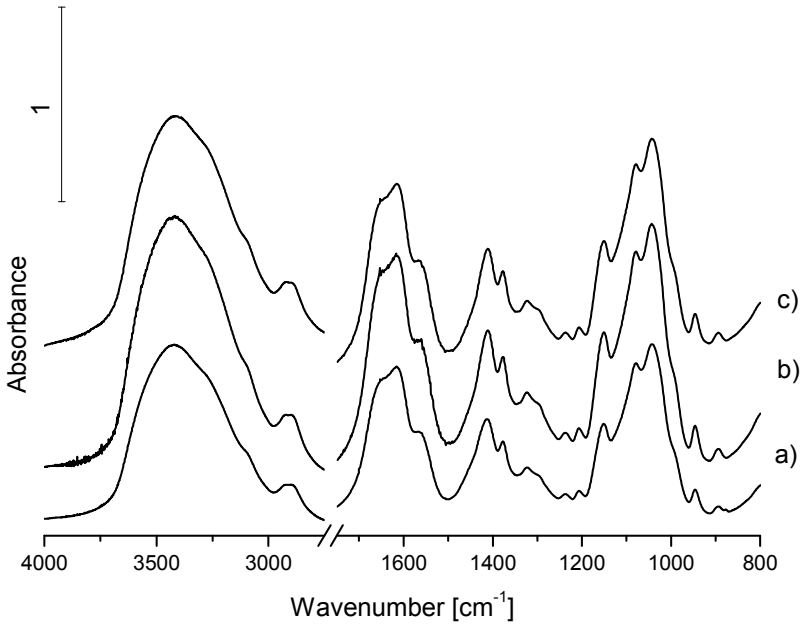

Fig. 1A

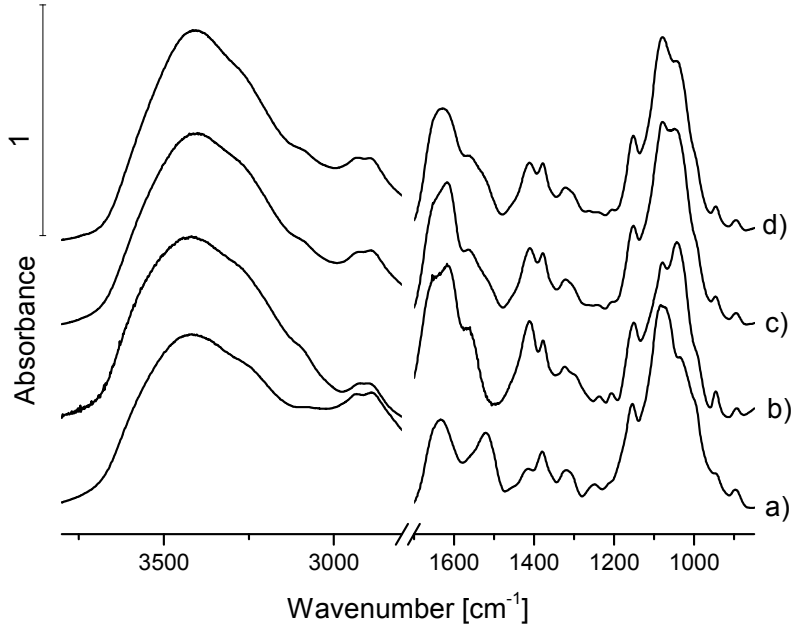

Fig. 1B

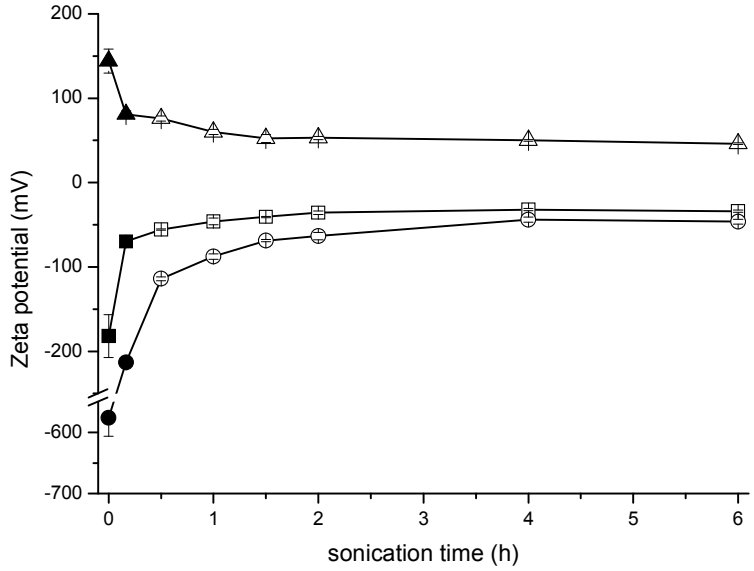
Zeta potential (mV)
200
100
0
-100
-200
-600
-700
0
1
2
3
4
5
6
sonication time (h)

Fig. 2A

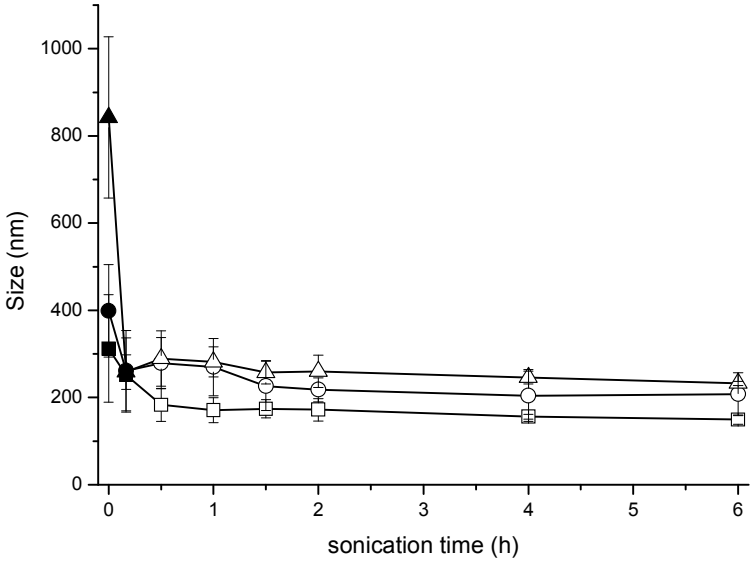
Size (nm)
1000
800
600
400
200
0
0
1
2
3
4
5
6
sonication time (h)

Fig. 2B

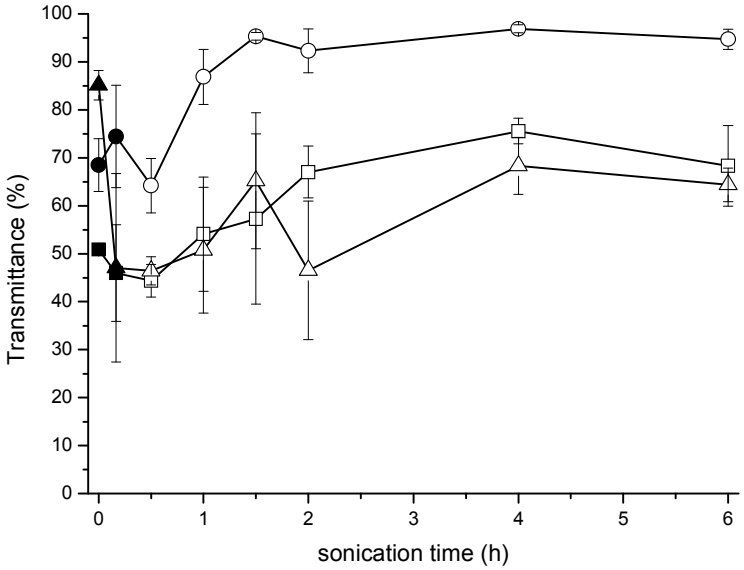
Transmittance (%)
sonication time (h)
0
10
20
30
40
50
60
70
80
90
100
0
1
2
3
4
5
6

Fig. 2C

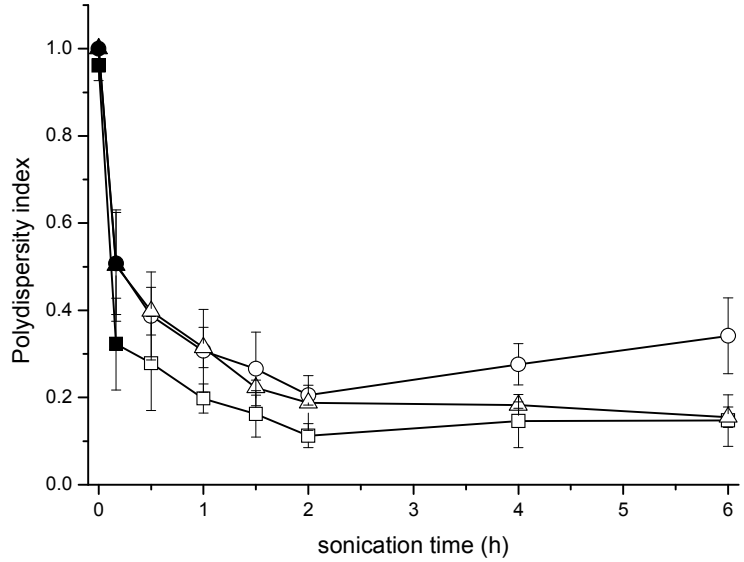
Polydispersity index
sonication time (h)
0.0
0.2
0.4
0.6
0.8
1.0
0
1
2
3
4
5
6

Fig. 2D

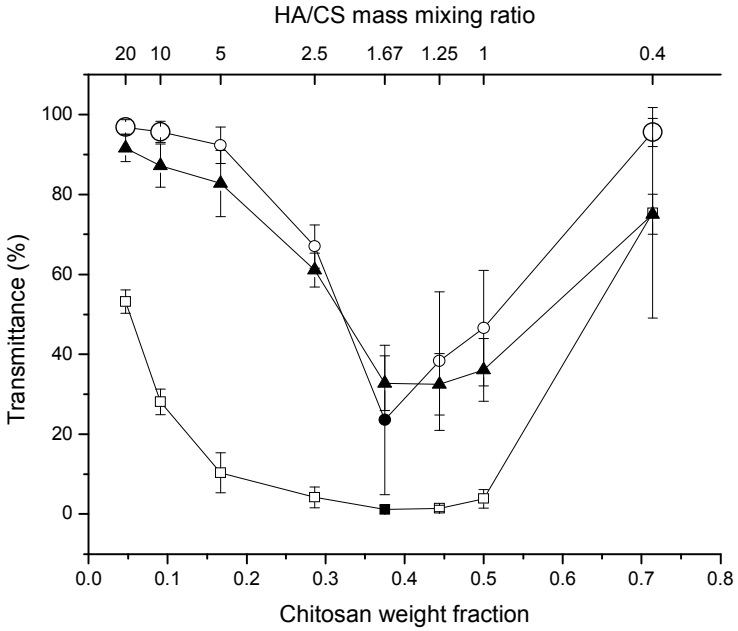
HA/CS mass mixing ratio
20 10 5 2.5 1.67 1.25 1 0.4
Transmittance (%)
Chitosan weight fraction

Fig. 4A

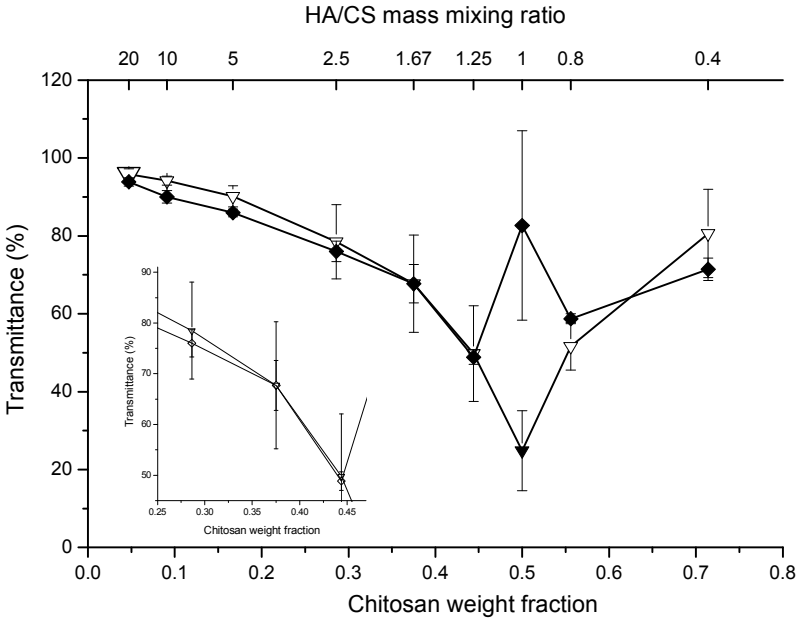
HA/CS mass mixing ratio
20 10 5 2.5 1.67 1.25 1 0.8 0.4
Transmittance (%)
Chitosan weight fraction

Fig. 4B

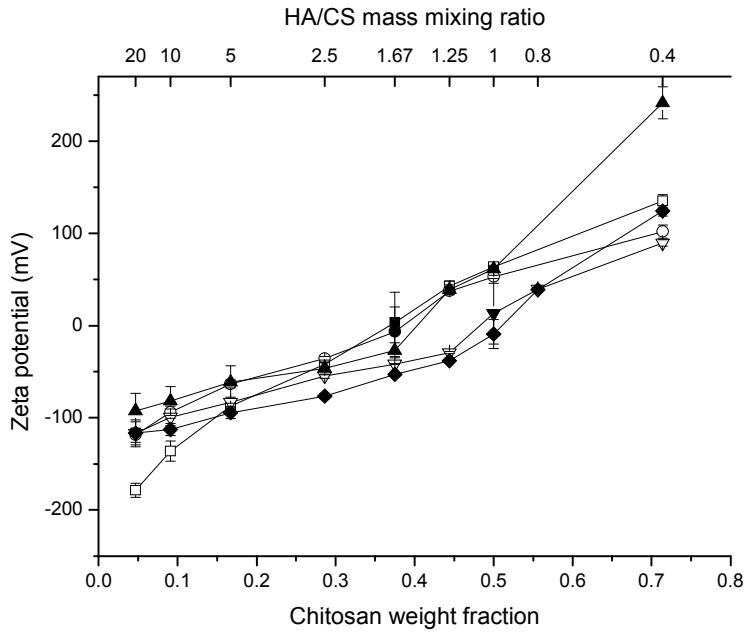
HA/CS mass mixing ratio
20 10 5 2.5 1.67 1.25 1 0.8 0.4
Zeta potential (mV)
200
100
0
-100
-200
0.0 0.1 0.2 0.3 0.4 0.5 0.6 0.7 0.8
Chitosan weight fraction

Fig. 5A

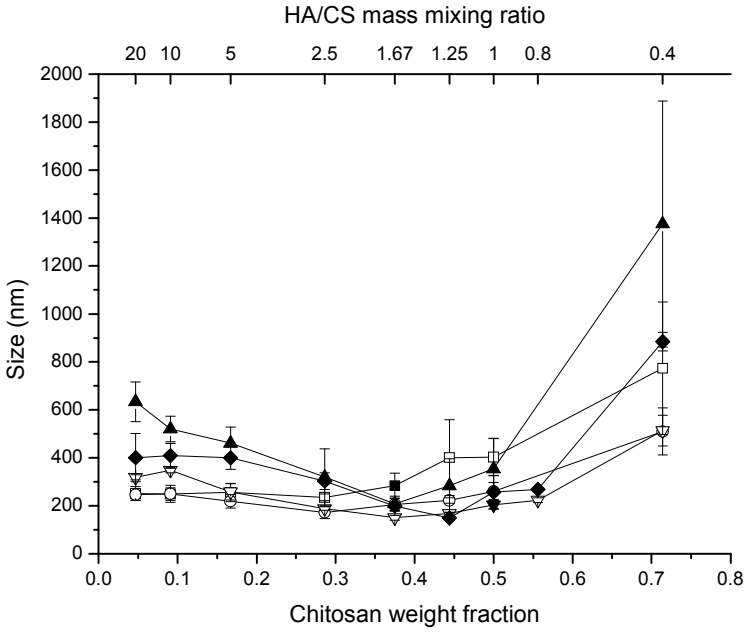
HA/CS mass mixing ratio
20 10 5 2.5 1.67 1.25 1 0.8 0.4
Size (nm)
2000
1800
1600
1400
1200
1000
800
600
400
200
0
0.0 0.1 0.2 0.3 0.4 0.5 0.6 0.7 0.8
Chitosan weight fraction

Fig. 5B

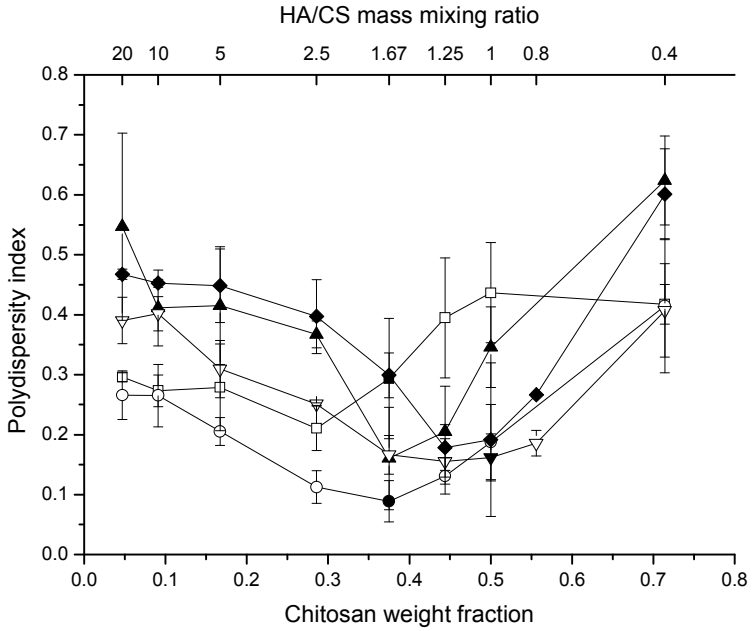
HA/CS mass mixing ratio
20 10 5 2.5 1.67 1.25 1 0.8 0.4
Polydispersity index
Chitosan weight fraction

Fig. 5C

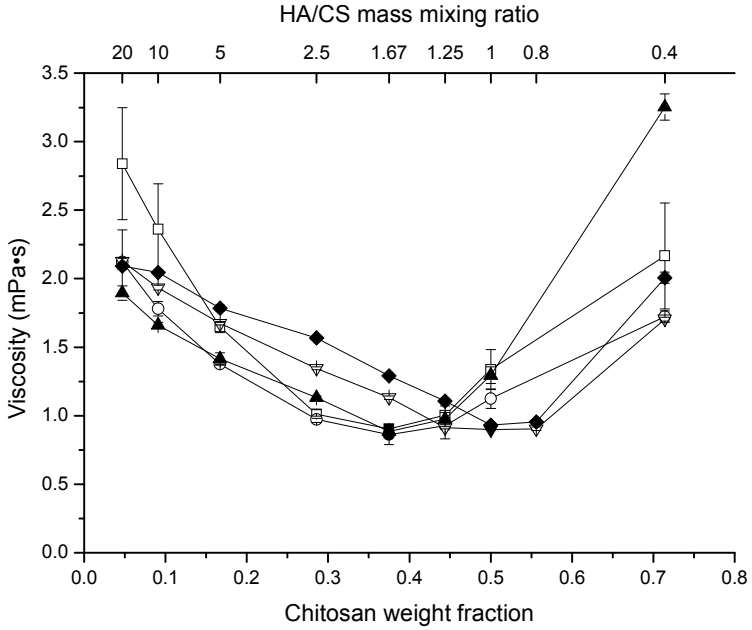
HA/CS mass mixing ratio
20 10 5 2.5 1.67 1.25 1 0.8 0.4
Viscosity (mPa•s)
Chitosan weight fraction

Fig. 5D

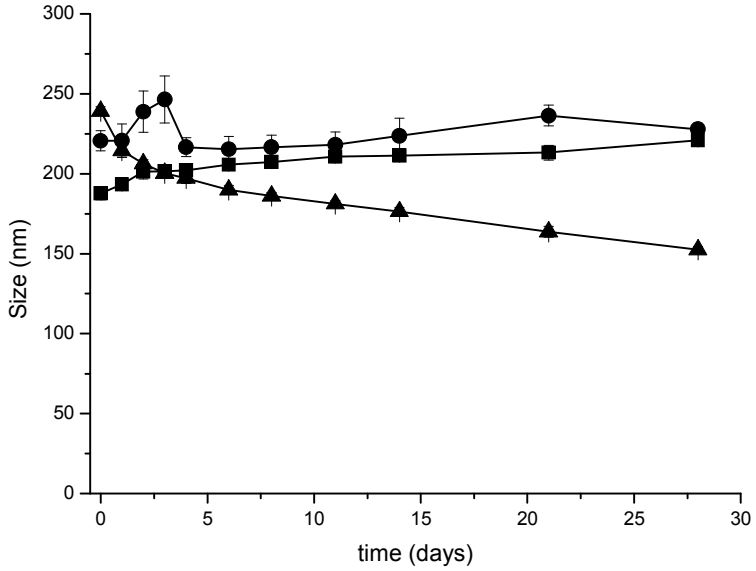
Size (nm)
time (days)
0
50
100
150
200
250
300
0
5
10
15
20
25
30

Fig. 7A

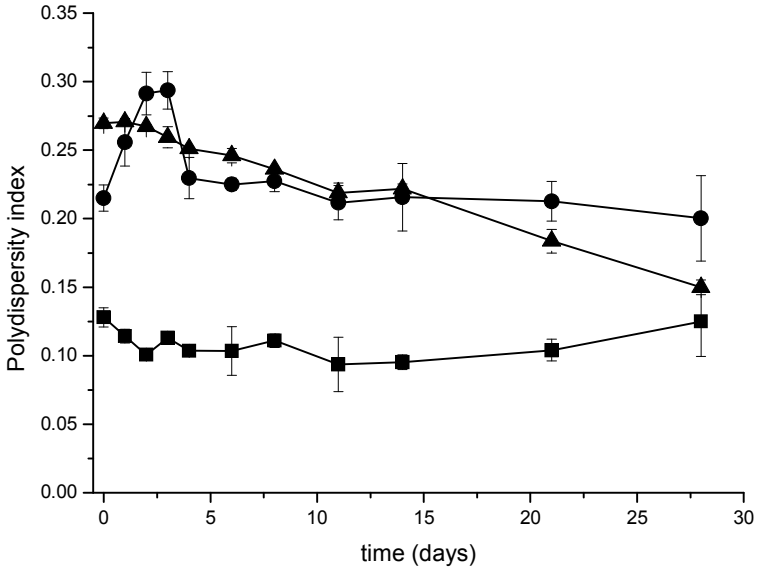
Polydispersity index
time (days)
0.00
0.05
0.10
0.15
0.20
0.25
0.30
0.35
0
5
10
15
20
25
30

Fig. 7B

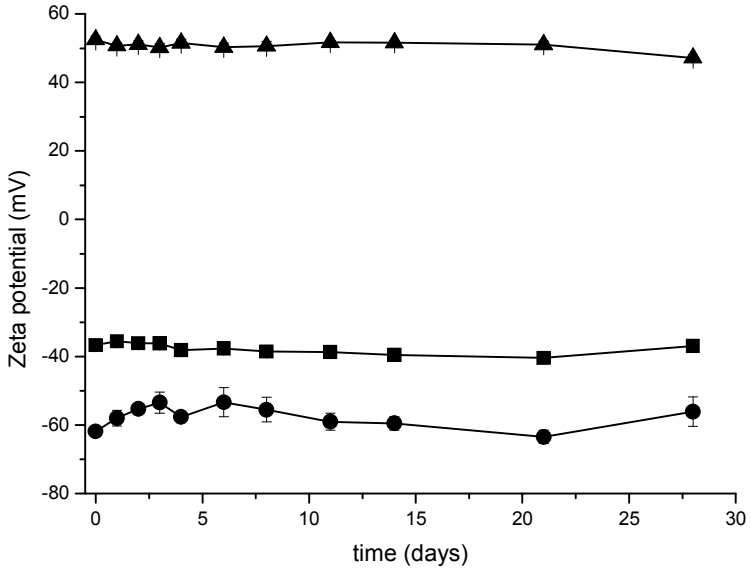

Fig. 7C

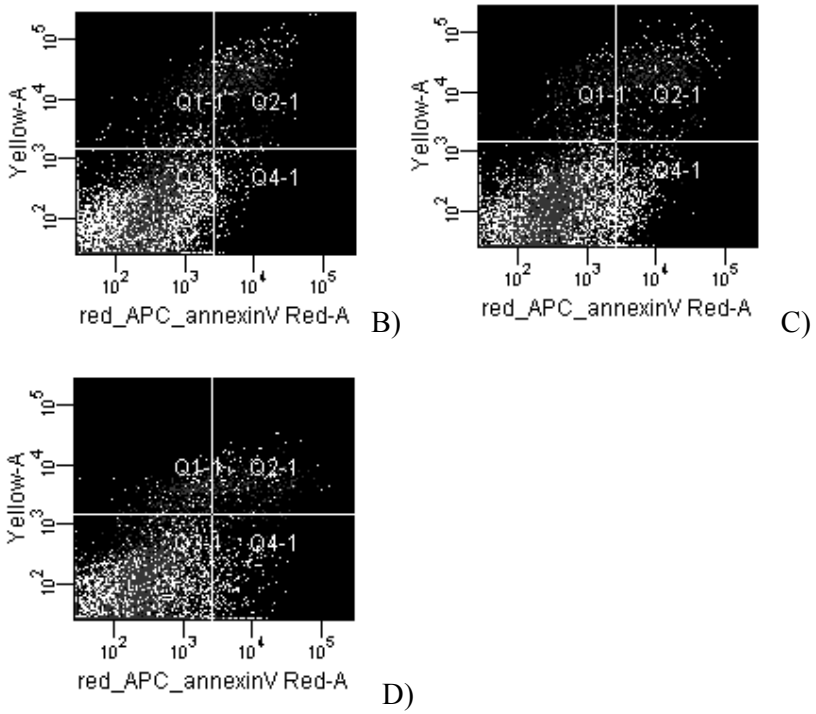

Fig. 8BCD

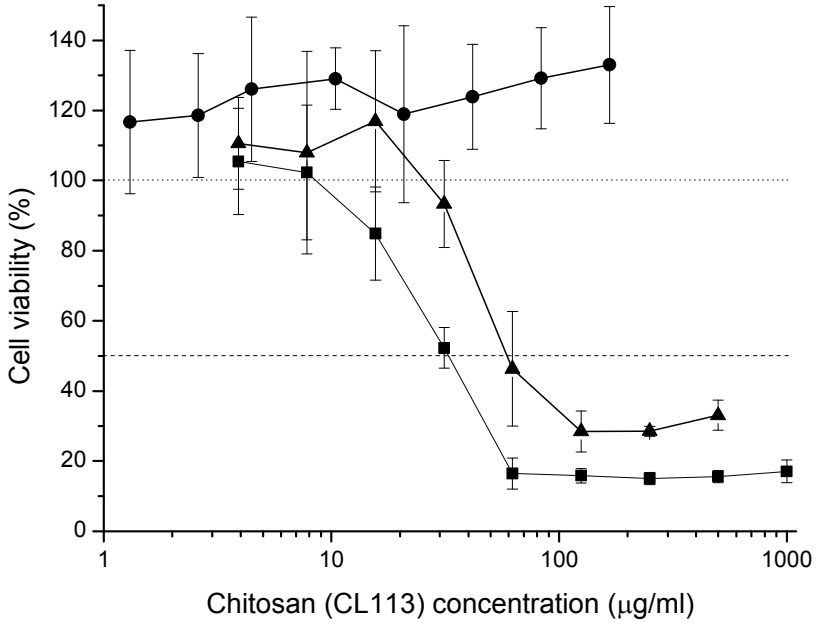
Cell viability (%)
0
20
40
60
80
100
120
140
1
10
100
1000
Chitosan (CL113) concentration (μg/ml)

Fig. 9